# Relationships between net primary productivity and forest stand age in U.S. forests

Liming He,[1] Jing M. Chen,[1] Yude Pan,[2] Richard Birdsey,[2] and Jens Kattge[3]

Received 11 August 2010; revised 17 June 2012; accepted 25 June 2012; published 3 August 2012.

[1] Net primary productivity (NPP) is a key flux in the terrestrial ecosystem carbon balance, as it summarizes the autotrophic input into the system. Forest NPP varies predictably with stand age, and quantitative information on the NPP-age relationship for different regions and forest types is therefore fundamentally important for forest carbon cycle modeling. We used four terms to calculate NPP: annual accumulation of live biomass, annual mortality of aboveground and belowground biomass, foliage turnover to soil, and fine root turnover in soil. For U.S. forests the first two terms can be reliably estimated from the Forest Inventory and Analysis (FIA) data. Although the last two terms make up more than 50% of total NPP, direct estimates of these fluxes are highly uncertain due to limited availability of empirical relationships between aboveground biomass and foliage or fine root biomass. To resolve this problem, we developed a new approach using maps of leaf area index (LAI) and forest age at 1 km resolution to derive LAI-age relationships for 18 major forest type groups in the USA. These relationships were then used to derive foliage turnover estimates using species-specific trait data for leaf specific area and longevity. These turnover estimates were also used to derive the fine root turnover based on reliable relationships between fine root and foliage turnover. This combination of FIA data, remote sensing, and plant trait information allows for the first empirical and reliable NPP-age relationships for different forest types in the USA. The relationships show a general temporal pattern of rapid increase in NPP in the young ages of forest type groups, peak growth in the middle ages, and slow decline in the mature ages. The predicted patterns are influenced by climate conditions and can be affected by forest management. These relationships were further generalized to three major forest biomes for use by continental-scale carbon cycle models in conjunction with remotely sensed land cover types.

**Citation:** He, L., J. M. Chen, Y. Pan, R. Birdsey, and J. Kattge (2012), Relationships between net primary productivity and forest stand age in U.S. forests, *Global Biogeochem. Cycles*, *26*, GB3009, doi:10.1029/2010GB003942.

## 1. Introduction

[2] The terrestrial carbon cycle is the most uncertain and variable component of the global carbon cycle [*Canadell et al.*, 2007; *Le Quéré et al.*, 2009]. Net primary productivity (NPP), the difference between gross primary production (GPP) and autotrophic respiration (AR) [*Chapin et al.*, 2006], is in turn the most variable part of the terrestrial carbon cycle [*Alexandrov et al.*, 1999], and greatly affects interannual variations of terrestrial carbon sinks [*Cramer et al.*, 1999]. NPP in forests is not only affected by climatic variability, but is also closely related to forest age. Typically, forest NPP increases rapidly at the early development stage, reaches a maximum in middle ages and gradually declines in later ages [*Bond-Lamberty et al.*, 2004; *W. J. Chen et al.*, 2002; *Wang et al.*, 2003; *Gower et al.*, 1996; *Pearson et al.*, 1987; *Pregitzer and Euskirchen*, 2004; *Ryan et al.*, 1997; *Wang et al.*, 2011]. However, *Kutsch et al.* [2009] found that a successional decline in NPP is not a 'universal feature' of natural forests and they identified several processes that work against such a decline. Given such complications, understanding the pattern of forest NPP associated with age is critically important for improving forest carbon cycle estimation [*Carey et al.*, 2001; *Chen et al.*, 2003; *Luyssaert et al.*, 2008; *Ryan et al.*, 1997; *Song and Woodcock*, 2003; *Yarie and Billings*, 2002]. Until now, large-scale carbon cycle modeling has not widely included forest stand-age information as an important variable [*Kohlmaier et al.*, 1995], although its first order effect was considered in regional carbon cycle modeling for Europe [*Zaehle et al.*, 2006], Canada [*Chen et al.*, 2003] and China [*Wang et al.*, 2007]. The reasons for the lack of consideration of forest age in estimating NPP may be lack of spatially explicit data

[1]Department of Geography and Program in Planning, University of Toronto, Toronto, Ontario, Canada.
[2]Newtown Square Corporate Campus, USDA Forest Service, Newtown Square, Pennsylvania, USA.
[3]Max Planck Institute for Biogeochemistry, Jena, Germany.

Corresponding author: L. He, Department of Geography and Program in Planning, University of Toronto, 100 St. George St., Room 5047, Toronto, ON M5S 3G3, Canada. (liming.he@gmail.com)


0886-6236/12/2010GB003942

of forest ages and the difficulty in determining NPP-age relationships for various forest types or tree species.

[3] It is impossible to directly measure forest NPP in the field in terms of this difference between GPP and AR [*Waring and Schlesinger*, 1985]. Alternatively, NPP can be defined as the total new organic matter produced during a specified interval, and can be estimated by combining (1) the amount of new organic matter assimilated and stored in plants (aboveground biomass increments in stems, branches, foliages etc., and belowground biomass increments in coarse and fine roots) and (2) the amount of assimilated organic matter that was lost (litterfall, dead roots, consumed by animals etc.) [*Clark et al.*, 2001] from which several minor NPP components can be omitted because of their relative insignificance (e.g., consumption by sap-suckers, emission of biogenic volatile compounds, organics leached from plant parts). In short, forest NPP is the net carbon product of trees that is allocated to several carbon pools- not only living biomass, but also soil organic matter. It is therefore a key flux in terrestrial carbon cycle modeling. Conventional forest inventories provide massive amounts of ground data about tree growth; however, they do not provide all necessary information for NPP estimation because the multiyear remeasurement period and sampling protocols that focus on tree stem allometry do not include measurement of foliage and fine root production. In spite of this limitation, forest inventory data have been used for estimating forest carbon stocks and stock changes over decades with an aggregated approach, often excluding full accounting of changes in soil carbon stocks associated with forest development. In many important applications, relevant ecosystem carbon pools are estimated with simple assumptions from ecosystem studies reported in the literature [*Fang and Wang*, 2001; *Heath et al.*, 2002; *Pan et al.*, 2011b]. In inventory-based forest carbon studies, one of the methods is to convert stem volume from inventories to total tree biomass increment and then to NPP for full carbon cycle estimation [*Kurz and Apps*, 1999]. However, the conversion from biomass increment to NPP is highly uncertain if only using inventory data (see also *W. J. Chen et al.* [2002]), which therefore affects the use of inventory data for improving carbon models that simulate a full carbon cycle including soil and vegetation components.

[4] Forest inventory data are insufficient for NPP estimation. Estimating forest NPP requires information about four components: (1) live biomass increment, (2) mortality, (3) foliage turnover, and (4) fine root turnover [*W. J. Chen et al.*, 2002]. Forest inventories can be effectively used for estimating only the first two terms [*Jenkins et al.*, 2001], yet the last two terms account for a large proportion of total NPP. For example, more than 50% of NPP in boreal forests is due to foliage and fine root production [*Gower et al.*, 1997]; about one third of NPP is allocated to foliage and a similar amount to fine root each year. Except for evergreen conifer forests with a foliage life-span of several years, foliage and fine roots are usually decomposed and emitted to the atmosphere or added to soil carbon pools within a year, and so these components cannot practically be included in forest inventory measurements. In previous studies [*W. J. Chen et al.*, 2002; *Jenkins et al.*, 2003; *Li et al.*, 2003], the estimates of foliage and fine root turnovers were made from limited empirical relationships between aboveground biomass and foliage or fine root biomass. These estimates are rather coarse mainly due to unknown variations of the turnover rates with stand age since such field information is rare [*Yanai et al.*, 2006], and cause the largest uncertainty in NPP estimates derived from forest inventory data. To resolve this issue, we used remote sensing data to provide additional information for estimating the foliage turnover rates, and empirical relationships to derive the fine root turnover rates. *Pan et al.* [2011a] compiled the first continental forest age map for North America (NA) at 1 km resolution. In this study the age map was used in combination with a yearly maximum Leaf Area Index (LAI) map of NA in 2000 at the same resolution [*Deng et al.*, 2006] to derive LAI-age relationships for eighteen major forest type groups in the United States (U.S.), where LAI is defined as the total one-sided (or one half of the total all-sided) green leaf area per unit ground surface area [*Chen and Black*, 1992]. We then combined the LAI-age relationships with species-specific leaf longevity and specific leaf area (SLA, leaf area per unit dry mass) to derive the foliage turnover rates at various stand ages for these forest type groups in the U.S. The relationships are also used for estimating the fine root turnover rates based on empirical relationships between fine root and leaf turnover rates.

[5] The objectives of our research are (1) developing NPP-age relationships for major forest biomes in the U.S. by combining data from Forest Inventory and Analysis (FIA), remote sensing, and species-specific traits in order to fill the data and knowledge gaps; and (2) examining whether there is a consistent pattern in the NPP-age relationships among all U.S. forest types and how critical the new information is for improving ecosystem models in terms of estimating forest carbon dynamics.

## 2. Data Sets

[6] Data sets derived from FIA forest inventories, remote sensing, and plant traits were used in this study to derive the NPP-age relationships for the U.S. (Table 1). All maps were re-projected to NA Albers Conical Equal Area projection at1 km resolution using nearest-neighbor re-sampling in the analysis.

### 2.1. Forest Inventory and Ecosystem Data

[7] FIA includes three sampling phases (http://www.fs.fed.us/). Phase 1 uses aerial photography and satellite data to characterize the acreage of forest and non-forest land in the U.S. Phase 2 consists of about 150,000 permanent field sample locations (approximately one plot every 6,000 acres) that are remeasured periodically to provide statistics on volume, biomass, harvest, growth, mortality, damage, species composition change, and site information such as ownership, stand age, and forest type. Phase 3 is a subset of phase 2 plots from which forest health data is collected, as well as data about woody debris, understory vegetation, and soils. At each sample location, a rigorous protocol from the FIA National Core Field Guide is followed to select sample plots and trees for measurements. For all phase 2 and 3 measurements, each FIA plot consists of a cluster of four circular subplots distributed over an acre in a fixed pattern. The millions of sampled trees from these plots provide the basis for estimating volume and biomass of live and dead trees in U.S. forests. Standing live biomass is estimated from

**Table 1.** Summary of Data Sets Used in This Study

| Data Set | Projection | Resolution | Range | Source |
|---|---|---|---|---|
| Forest Age Map | NA Albers, NAD 83 | 1 km | 0–888 yrs | *Pan et al.* [2011a] |
| Leaf Area Index Map | Lon/lat degree | ~1 km | 0–10 | *Deng et al.* [2006] |
| Forest Type Map | Albers Conical Equal Area | 250 m | 141 type and 28 type group | *Ruefenacht et al.* [2008] |
| VCF Map[a] | Lon/lat degree | ~500 m | 0–80% | *Hansen et al.* [2007] |
| Land Cover | Lon/lat degree | ~1 km | 23 cover types | *Global Vegetation Monitoring Unit* [2003] |
| Carbon Stock Table | | | 51 tables over 10 U.S. regions | *Smith et al.* [2006] |
| Plant Traits | | Individual measurements and species specific data | | *Kattge et al.* [2011], *White et al.* [2000, 2002] |

[a]VCF = Vegetation Continuous Fields.

the measurements of trees greater than 2.5 cm in dbh (diameter at breast height) using a standard set of biomass equations covering all tree components [*Jenkins et al.*, 2003].

[8] Live biomass includes coarse roots (greater than 0.2 to 0.5 cm), stems, branches, and foliage. The biomass of standing dead trees is estimated using the same equations as for living trees with adjustments for biomass loss [*Smith et al.*, 2003]. In addition, understory biomass which includes tree seedlings less than 2.5 cm dbh is estimated using data from field studies [*Birdsey*, 1996], and coarse woody debris is estimated using field measurements of carbon density, decay rates, and estimates of logging residues [*Smith et al.*, 2006].

[9] The forest ecosystem carbon yield tables derived from the U.S. inventory plot data [*Smith et al.*, 2006] provide stand-level merchantable volume and carbon stocks in forest ecosystems at different age classes for 18 forest type groups within 10 ecoregions of the United States. The stand ages of inventory sample plots were usually determined by sampled tree ring cores that represent the average age of the trees on the sample plot. The plots that were not given an age in the forest inventory, such as multiaged plots, were assigned an "equivalent age" based on volume and stocking. About 10% of all inventory sample plots are considered multiaged [*Smith et al.*, 2009].

[10] In total, 102 forest carbon yield tables are available, of which 51 represent afforestation of nonforest sites and 51 reforestation of harvested forest sites. The tables include six distinct carbon pools in forest ecosystems for the different forest types and age classes: (1) live trees, (2) standing dead trees, (3) understory vegetation, (4) down dead wood, (5) forest floor, and (6) soil organic carbon. The last three carbon pools in afforestation sites are different from reforestation sites because of the effect of post-harvest residuals. We used the afforestation tables in this study because we excluded post-harvest residual (the down dead wood) [*Smith et al.*, 2006, Appendix B] that may distort true forest NPP growth patterns.

[11] These tables represent the majority of forest conditions in the U.S., and age classes up to 90 years in the southern regions and 125 years elsewhere. There is insufficient inventory data to characterize forests with stand ages beyond these limits. Although for some U.S. forest types an age of 125 is young compared to their life expectancies [*Pan et al.*, 2011a], there is little (about 1% of area) old growth forest remaining in U.S. due to past intensive land use and forest management [*Lichstein et al.*, 2009]. This small area does not represent significant contribution to the overall NPP of U.S. forests, although it may be locally relevant. The estimates in the look-up tables are called "average estimates," because these tables represent averages of carbon stocks over large areas of each eco-region.

### 2.2. Forest Stand Age and Uncertainty Maps

[12] *Pan et al.* [2011a] compiled the first continental forest age map of NA by combining forest inventory data, historical fire data, and optical satellite data including the data set from NASA's LEDAPS project [*He et al.*, 2011; *Masek et al.*, 2008]. The availability of this map with 2000 as the base year makes it possible to analyze the LAI - age relationships. Observed tree age or time since a known disturbance are commonly used to estimate forest ages [*Bradford et al.*, 2008]; these two kinds of ages are both included in the map. If natural disturbances or harvesting do not kill or remove all of the trees in a forest stand, there is a difference between observed (and averaged) forest age and a surrogate age based on time since disturbance [*Bradford et al.*, 2008; *Pan et al.*, 2011a]. Since we cannot differentiate the type of ages in the map, errors may be introduced to the LAI – age relationships which will be discussed in section 4. The age map represents the dominant forest age in each pixel interpolated by Voronoi polygons from plot age data. The standard deviation of each 1-km pixel of the age map was calculated based on 16 sub-pixels [*Pan et al.*, 2011a]. Uncertainty of forest ages is less for the U.S. eastern forests than the western forests because of relatively less diverse age structures there.

### 2.3. Land Cover

[13] The land cover map was downloaded from the Global Land Cover 2000 Project, which produced this data set using the SPOT4 VEGETATION (VGT) product [*Global Vegetation Monitoring Unit*, 2003]. The map includes 23 land cover types and 3 forest biome types: deciduous broadleaf forest (DBF), evergreen needleleaf forest (ENF), and mixed forest (MF). This map was used in the LAI algorithm [*Chen et al.*, 2006; *Deng et al.*, 2006].

### 2.4. Leaf Area Index Map

[14] A data set of LAI in NA was produced using the SPOT4 VGT 10-day synthesis product for 12 months in 2000 using the original LAI algorithm (version 1) in which the LAI maximum is set to 6.0 for deciduous forest in order to avoid saturation in reduced simple ratio (RSR) signals [*Chen et al.*, 2006; *Deng et al.*, 2006]. We also produced two new data sets without setting a maximum LAI threshold: one data set (version 2) is unsmoothed, and another data set

(version 3) is smoothed using the algorithm developed by *Chen et al.* [2006].

[15] Another LAI data set from the MODIS (MODerate Resolution Imaging Spectroradiometer) monthly LAI product (collection 5) in 2000 was also used [*Yang et al.*, 2006].

### 2.5. Vegetation Continuous Field Map

[16] The MODIS Vegetation Continuous Fields (VCF) product (collection 4, version 3) was used to screen pixels with small forest percent cover at the sub-pixel level in order to reproduce the correct LAI-age curve [*Hansen et al.*, 2007, 2002, 2003]. The valid values of this product range from 0 to about 80% representing the percentage of tree cover at 500-m MODIS pixels for all land cover types.

### 2.6. Forest Type Map

[17] A forest type map from the USDA Forest Service was used in deriving LAI-age relationships for the forest type groups [*Ruefenacht et al.*, 2008]. Overall map accuracy for the classification of the 28 forest type groups was 69%. Some forest type groups are less dominant and have limited sample plots, so only 18 are included in the carbon stock tables [*Smith et al.*, 2006]. It is possible there are mismatched pixels of forest or forest type between the forest type and land cover maps (DBF, ENF or MF) because of their different data sources and co-registration errors.

### 2.7. Plant Trait Data

[18] SLA, the foliage turnover ratio ($t_l$) and the ratio of new root carbon to new leaf carbon allocation ($R_{fr,l}$) were used to determine leaf biomass, and leaf and root turnover rates. Individual observations of SLA were provided by the TRY initiative [*Kattge et al.*, 2011]. About 3000 SLA records for the tree species of interest in NA are collected in the TRY database. Species-specific information for leaf longevity, which determines the foliage turnover ratio, and the ratio of new root carbon to new leaf carbon allocation were obtained from *White et al.* [2000].

## 3. Methods

[19] We estimated NPP (t C ha$^{-1}$ year$^{-1}$) as the sum of biomass increments or turnovers of several components [*W. J. Chen et al.*, 2002]:

$$NPP = \Delta B + M + L_l + L_{fr} \quad (1)$$

where $\Delta B$ is the increment in the total living biomass (the sum of increments in stem, branch and coarse root, as foliage and fine root do not change much from year to year), $M$ is the mortality including only the stand dead tree and the down dead wood, $L_l$ is the turnover of foliage, and $L_{fr}$ is the turnover of fine root in soil.

[20] We used the following steps to estimate the four NPP components. (1) Pre-processing was used to get plant traits data for 18 forest types and three major forest biomes. (2) $\Delta B$ and $M$ were estimated using carbon stock tables. (3) LAI-age relationships were derived and then $L_l$ was estimated using LAI and plant trait data. (4) $L_{fr}$ was estimated using the empirical relationship between $L_l$ and plant trait data. (5) The NPP and age relationship was fitted, and (6) the uncertainty of total NPP was also estimated.

### 3.1. Pre-processing for Plant Trait Data

[21] We assumed that the three plant traits (SLA, $t_l$, and $R_{fr,l}$) are age-invariable due to the limited records. We took the following steps to estimate each plant trait:

[22] 1. We searched the plant trait records provided by the TRY database, which were collected from different publications, for forest types in Table 1 of *Ruefenacht et al.* [2008]; we then estimated average values of the plant trait variables for forest types based on the records of tree species in forest type categories.

[23] 2. We classified the records into several forest type groups: fir, spruce, pine, hemlock, oak and other deciduous broadleaf forest, and calculated the mean values for each group.

[24] 3. We counted the pixels for each forest type in Table 1 of *Ruefenacht et al.* [2008] to determine the area weight of its forest type group. The average plant trait values from step 1 were assigned to corresponding forest types; for those types without corresponding plant trait values, we used the group average from step 2. We obtained the weighted plant trait value for each forest type group according to the area weight and plant trait value of each type, and were able to estimate specific plant trait values for each forest type group.

### 3.2. Determining the First and Second Components of NPP

[25] The carbon stock estimates of live tree, standing dead tree, and down dead wood from the tables [*Smith et al.*, 2006] were used to estimate the first and second components ($\Delta B$ and $M$) of forest NPP. The increment in the total biomass carbon (t C ha$^{-1}$ year$^{-1}$) was determined by dividing the difference between two live tree biomasses by the time interval between them, for each time interval in the table. Assuming that the foliage biomass does not change from year to year, this total biomass increment includes only the increments of stems, branches and coarse roots, but does not include the turnover of foliage and fine roots. The total mortality is considered to be the sum of the increments in standing and down dead trees, which can be calculated in the same way as the increment in the total living biomass.

### 3.3. Determining the Foliage Turnover

#### 3.3.1. Defining the Relationship Between Maximum LAI and Forest Age

[26] Maximum foliage biomass (including the understory) corresponds to the maximum LAI during a year. The maximum LAI values for each pixel were extracted by searching the seasonal trajectories of LAI values in each LAI product to produce the maximum LAI map. We found that the maximum LAI for the U.S. mostly occurred (peaked) in the last 10-days of July.

[27] We used five years for age group intervals (0–2.5 yrs, 2.5–7.5 yrs, and so on), searched all the maximum LAI values associated with stand ages that have low uncertainties (by std-age map) in the same age group for each forest type group or each major forest biome, and then took their averages to derive the LAI-age relationships. The five-year age groups are same as the age groups in the carbon stock table. We tested smaller steps less than 5 years but the relationships became

noisy. The GLC2000 land cover map was used to derive LAI-age relationships for deciduous broadleaved forest (DBF, land cover code 1 and 2), evergreen needle-leaved forest (ENF, land cover code 4 and 5), and mixed forest (MF, land cover code 6) in NA because it explicitly includes a mixed forest type (broadleaved and needleleaved) not included in the USFS forest type map.

#### 3.3.2. Separating Canopy LAI and Understory LAI

[28] The total LAI ($LAI_t$) retrieved by Deng's algorithm [*Deng et al.*, 2006] consists of LAI from both the tree canopy ($LAI_f$) and the understory (from shrubland and grass - $LAI_u$):

$$LAI_t = LAI_u + LAI_f \tag{2}$$

Generally, the understory LAI dominates immediately after disturbances or in the beginning of afforestation; then when trees grow larger and compete for space and sunlight, the understory LAI decreases gradually. The relationship between the proportions of $LAI_u$ and $LAI_f$ (or sometimes $NPP_u$ and $NPP_f$) change with forest stand age. For example, *W. J. Chen et al.* [2002] assumed that the understory NPP decreases exponentially with forest stand age. To accurately quantify the NPP-age relationship, we developed an approach to separate $LAI_f$ and $LAI_u$ from the LAI-age relationship and used $LAI_f$ and plant traits data to estimate foliage turnover.

[29] $LAI_u$ and $LAI_f$ are two unknowns. We assumed that the $LAI_u$ is proportional to the direct radiation reaching the ground (or the $LAI_u$ is proportional to the gap fraction):

$$LAI_u = LAI_{u,\max} \exp\left(\frac{-k(\theta)\Omega LAI_f}{\cos(\theta)}\right) \tag{3}$$

where $LAI_{u,\max}$ is the maximum understory LAI right after disturbance or afforestation in a well-developed forest ecosystem with abundant nutrition for understory vegetation; $\theta$ is the daily average solar zenith angle (we set it 60 degrees in this study); $k(\theta)$ is the project coefficient relating to leaf angular distribution (we assume it is spherical leaf distribution, and set it to 0.5); and $\Omega$ is the clumping index from *Chen et al.* [2005] for each forest type groups. $LAI_u$ is set to its minimum value when the ecosystem has maximum LAI (generally when the canopy reaches closure).

[30] We initialized $LAI_{u,\max}$ using the value of $LAI_t$ (the average $LAI_t$ for ages from 0 yr to 2.5 yrs) for stand-age zero in the LAI-age curves. The value of $LAI_{u,\max}$ could be overestimated. However, this assumption only facilitates setting the initial value of $LAI_f$ to zero for stand-age zero in order to construct the $LAI_f$-age relationships, and may not be problematic because a pure forest pixel of stand age zero rarely exists at 1 km resolution.

[31] We defined the peak NPP age of a forest stand to be when the LAI value reaches an obvious peak in the LAI-age curves. If a peak NPP age is unidentifiable from LAI, the age for the maximum biomass NPP (section 3.2) is used with an assumption that the LAI generally peaks when NPP peaks.

[32] In short, there are 3 steps to determine the LAI curve for a young growing forest before reaching the peak NPP age: (1) $LAI_f$ linearly increases from zero to the peak value; (2) The first order estimation of $LAI_u$ is made using equation (3); and (3) $LAI_f$ is obtained as the difference of $LAI_t$ and $LAI_u$ from step 2 (equation (2)). These three steps can effectively separate $LAI_t$ into a persistent increase of $LAI_f$ and a persistent decrease of $LAI_u$, reflecting a realistic dynamic pattern of LAI in forest.

[33] To solve $LAI_f$ after the forest reaches the peak age, we let $a = LAI_{u,\max}$, $b = -k(\theta)\cdot\Omega/\cos(\theta)$ and substitute the $LAI_u$ in equation (2) using equation (3):

$$LAI_f = LAI_t + Lambertw(0, -(\mathrm{a}\cdot\mathrm{b})/\exp(\mathrm{b}\cdot LAI_t))/b \tag{4}$$

where Lambertw is the Lambert $W$ function, and Lambertw (0, x) is the 0-th branch of this multivalued function [*Corless et al.*, 1996]. At a given age, if the function has no real solution for separating the $LAI_t$ we then assign $LAI_u$ to a value according to field measurement from references in the literature.

#### 3.3.3. Foliage Turnover

[34] We calculated the foliage turnover rate ($L_l$) using the maximum forest canopy LAI ($LAI_f$) and parameters based on plant trait data:

$$L_l = LAI_f/SLA \cdot t_l \cdot c \tag{5}$$

where $L_l$ is in t C $ha^{-1}$ $yr^{-1}$; SLA is in units of ha $t^{-1}$; $t_l$ is foliage (to litter) turnover ratio ($yr^{-1}$) that differs for forest types; and $c$ is the ratio of carbon to dry matter. The dry matter of tree leaves contains from 45 to 50% carbon [*Reichle et al.*, 1973; *Schlesinger*, 1997], and we assume $c$ = 0.5 [*Pregitzer and Euskirchen*, 2004].

### 3.4. Determining Fine Root Production

[35] Live root biomass is proportional to stand density and LAI [*DesRochers and Lieffers*, 2001], thus we can estimate fine root production from stand LAI. Fine root turnover rate is linked to the foliage turnover rate by introducing the index $R_{fr,l}$:

$$L_{fr} = R_{fr,l} \cdot L_l \tag{6}$$

We discussed uncertainty in $R_{fr,l}$ in section 5.1.

### 3.5. NPP-Age Relationships

[36] The total NPP and age relationship was fitted using equation (7) [*Chen et al.*, 2003]:

$$NPP(age) = a\left(1 + \frac{b\left(\frac{age}{c}\right)^d - 1}{e^{\left(\frac{age}{c}\right)}}\right) \tag{7}$$

where a, b, c, and d are the coefficients to be determined, and age is a variable.

### 3.6. Methods of Uncertainty Analysis

[37] The absolute error of total NPP ($\sigma_{NPP}$, given as a standard deviation) in equation (1) for a five-year age group is calculated as [*Bevington and Robinson*, 2003]

$$\sigma^2_{NPP} = \sigma^2_{\Delta B} + \sigma^2_M + \sigma^2_{L_l+L_{fr}} \tag{8}$$

The three variables on the right side of equation (8) are from independent measurements and assumed to be uncorrelated

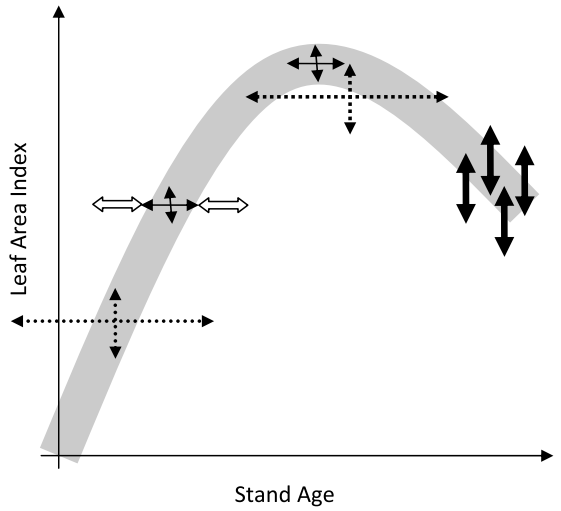


**Figure 1.** Analysis of errors in the LAI-age relationship using an exaggerated LAI-age curve. In this study, we calculated the average and one standard deviation (vertical double arrow in solid and thin lines) of LAI within a narrow age bin indicated by the horizontal double arrow in solid and thin lines. If there are no errors in age and LAI, the deviation is only from spatial variation of forest. If there are errors in the forest age map, equivalently we estimated the average and one standard deviation of LAI (vertical double arrow in dash line) within an enlarged age bin indicated by the horizontal double arrow in dash line; we concluded that the one standard deviation will became bigger, but the average of LAI doesn't change significantly, except around the maximum of LAI (causing a bias). If there are errors in the LAI product as shown by the thick and solid arrows, extra variation will be added to the one standard deviation. In short, both forest spatial variation and errors in the LAI product and forest stand age map can contribute to the deviation of LAI in an age bin, and their effects cannot be separated. The hollow arrows demonstrate the ranges (average of one standard deviations of stand ages within a narrow age bin from the stand age quality map) to calculate $LAI_{f,-\sigma_a}$ and $LAI_{f,+\sigma_a}$ in equation (13).

within the narrow age range and with zero covariance. $L_l$ and $L_{fr}$ are correlated in the calculation and their error is estimated by

$$\sigma^2_{L_l+L_{fr}} = \sigma^2_{L_l} + \sigma^2_{L_{fr}} + 2 \cdot \mathrm{cov}_{L_l,L_{fr}} \tag{9}$$

where $\mathrm{cov}_{L_l,L_{fr}}$ is for covariance and cannot directly be estimated from the data. We simplified it as $\mathrm{cov}_{L_l,L_{fr}} \approx \mathrm{cov}_{L_l,R_{fr,l}\cdot L_l} = R_{fr,1}\cdot\mathrm{cov}_{L_l,L_l} = R_{fr,1}\cdot\sigma^2_{L_l}$.

[38] Because $LAI_f$, $SLA$, $t_l$, $c$ and $R_{fr,1}$ are uncorrelated, so we only need to estimate $\sigma_{L_l}$ and $\sigma_{L_{fr}}$ respectively as

$$\left(\frac{\sigma_{L_l}}{L_l}\right)^2 = \left(\frac{\sigma_{LAI_f}}{LAI_f}\right)^2 + \left(\frac{\sigma_{SLA}}{SLA}\right)^2 + \left(\frac{\sigma_{t_l}}{t_l}\right)^2 + \left(\frac{\sigma_c}{c}\right)^2 \tag{10}$$

$$\left(\frac{\sigma_{L_{fr}}}{L_{fr}}\right)^2 = \left(\frac{\sigma_{L_l}}{L_l}\right)^2 + \left(\frac{\sigma_{R_{fr,l}}}{R_{fr,l}}\right)^2 \tag{11}$$

The error of LAI, $\sigma_{LAI_f}$, in the LAI-age curve is from two sources: the error from the LAI algorithm and the error the forest stand age map (Figure 1). $\sigma_{LAI_f}$ is approximated as

$$\sigma^2_{LAI_f} = \sigma^2_{LAI_s} + \sigma^2_{LAI_a} \tag{12}$$

where $\sigma_{LAI_s}$ is one standard deviation of LAI for the age group, which includes the deviations caused by spatial variation of LAI, LAI algorithm error and forest age error; and $\sigma_{LAI_a}$ is a bias of the LAI average caused by the error of stand age. We estimated $\sigma_{LAI_a}$ in an indirect way:

$$\sigma_{LAI_a} = \max(abs(LAI_f - LAI_{f,+\sigma_a}), \mathrm{abs}(LAI_f - LAI_{f,-\sigma_a})) \tag{13}$$

where $LAI_f$ is the average LAI for an age group, $\sigma_a$ is the average of one standard deviations of ages (from the age uncertainty map) for the $LAI_f$ age group, $LAI_{f,-\sigma_a}$ and $LAI_{f,+\sigma_a}$ are biased LAIs due to the age biases of $\pm\sigma_a$.

[39] The mean value ($E$%) for relative error of NPP ($\sigma_{NPP}$/NPP·100) for all ages of a forest type is reported in the results section.

## 4. Results

### 4.1. The Three Plant Traits for U.S. Forest

[40] The SLAs and their corresponding standard errors for several tree species and several forest types are listed in Tables 2a and 2b.

[41] The foliage turnover ratios show distinct differences among various forest types due to their different foliage longevity (Appendix A.1.1 in *White et al.* [2000]). The foliage turnover ratios for 15 forest types are listed in Table 3a. The averages of the ratios for four groups (fir, spruce, pine, and hemlock) are listed in Table 3b.

[42] The results for fine root turnover ratio ($R_{fr,l}$) are listed in Tables 4a, 4b, and 5. *White et al.* [2000] found that the $R_{fr,l}$ value for ENF was the only case with extreme skewness, with the mean value (2.7) almost twice the median (1.4). The apparent reason is that some firs have extremely high $R_{fr,l}$ (larger than 10). However, through an examination of data provided by *Vogt et al.* [1982], *Grier et al.* [1981], and *Fogel* [1983], we found that they explicitly included the mycorrhiza in the fine root product. Therefore, these outliers were excluded in our estimation of $R_{fr,l}$. The spruce group has only one sample and it is merged with the fir group. We assigned the value of $R_{fr,l}$ for hemlock, tamarack, and cedar with the average (1.59) of fir, spruce, and pine due to insufficient data. Our results for $R_{fr,l}$ for ENF are very close to the median values (1.4) provided by *White et al.* [2000].

[43] We labeled forest type groups in the conifer biome with codes from 100 to 400, and in the deciduous biome with codes from 500 to 920. The foliage turnover ratio is set to 1.0 for deciduous broad-leaved forests. The weighted rates for 18 forest type groups are listed in Table 5.

### 4.2. The NPP Components $\Delta B$ and $M$

[44] After checking the 51 tables and the forest type map, we found that each forest type group is generally located within one to five geographically adjacent regions, and each forest type group dominates one or two adjacent regions. Accounting for the regional adjacency of each forest type group and for the purpose of general applications, we

**Table 2a.** Specific Leaf Area ($m^2$ $kg^{-1}$) for Several Forest Types[a]

| Forest Type Code[b] | Dominant Tree Species | Latin Names | SLA ± std | Samples |
|---|---|---|---|---|
| 101 | Jack Pine | *Pinus banksiana* | 5.2 ± 1.6 | 2 |
| 102 | Red Pine | *Pinus resinosa* | 3.4 ± 1.1 | 8 |
| 103 | Eastern White Pine | *Pinus strobus* | 5.2 ± 2.5 | 9 |
| 121 | Balsam Fir | *Abies balsamea* | 5.3 ± 0.9 | 21 |
| 122 | White Spruce | *Picea glauca* | 3.4 ± 1.4 | 5 |
| 123 | Red Spruce | *Picea rubens* | 3.5 | 1 |
| 125 | Black Spruce | *Picea mariana* | 3.8 ± 1.5 | 8 |
| 127 | Northern Whitecedar | *Thuja occidentalis* | 4.9 ± 1.1 | 7 |
| 141 | Longleaf Pine | *Pinus palustris* | 3.3 ± 0.5 | 32 |
| 142 | Slash Pine | *Pinus elliottii* | 3.6 ± 0.8 | 30 |
| 161 | Loblolly Pine | *Pinus taeda* | 6.1 ± 2.2 | 88 |
| 164 | Sand Pine | *Pinus clausa* | 6.7 ± 1.6 | 29 |
| 166 | Pond Pine | *Pinus serotina* | 3.6 | 1 |
| 167 | Pitch Pine | *Pinus rigida* | 4.9 | 1 |
| 168 | Spruce Pine | *Pinus glabra* | 8.7 ± 2.0 | 26 |
| 181 | Red (or Eastern) Cedar | *Juniperus virginiana* | 1.7 ± 0.4 | 20 |
| 201 | Douglas-Fir | *Pseudotsuga menziesii* | 6.5 ± 2.6 | 10 |
| 221 | Ponderosa Pine | *Pinus ponderosa* | 2.5 ± 1.4 | 12 |
| 223 | Jeffrey Pine | *Pinus jeffreyi* | 3.0 ± 0.0 | 4 |
| 267 | Grand Fir | *Abies grandis* | 4.7 | 1 |
| 268 | Subalpine Fir | *Abies lasiocarpa* | 3.9 ± 0.0 | 2 |
| 269 | Blue Spruce | *Picea pungens* | 2.1 | 1 |
| 281 | Lodgepole Pine | *Pinus contorta* | 3.8 ± 0.6 | 4 |
| 301 | Western Hemlock | *Tsuga heterophylla* | 13.4 ± 5.4 | 11 |
| 305 | Sitka Spruce | *Picea sitchensis* | 5.3 ± 1.7 | 109 |
| 364 | Monterey Pine | *Pinus radiata* | 6.3 ± 1.5 | 38 |
| 366 | Limber Pine | *Pinus flexilis* | 2.7 | 1 |
| 384 | Norway Spruce | *Picea abies* | 5.1 ± 3.0 | 125 |
| 405 | Southern Red Oak | *Quercus falcata* | 12.4 ± 1.7 | 30 |
| 501 | Post Oak | *Quercus stellata* | 7.0 | 1 |
| 502 | Chestnut Oak | *Quercus prinus* | 12.4 ± 4.1 | 5 |
| 504 | White Oak | *Quercus alba* | 13.1 ± 3.5 | 11 |
| 505 | Northern Red Oak | *Quercus rubra* | 16.1 ± 4.4 | 56 |
| 509 | Bur Oak | *Quercus macrocarpa* | 17.4 ± 8.3 | 29 |
| 510 | Scarlet Oak | *Quercus coccinea* | 10.7 ± 1.6 | 2 |
| 513 | Black Locust | *Robinia pseudoacacia* | 19.4 ± 6.8 | 12 |
| 601 | Swamp Chestnut Oak | *Quercus michauxii* | 18.8 ± 3.2 | 31 |
| 701 | Black Ash | *Fraxinus nigra* | 23.3 ± 7.6 | 5 |
| 703 | Swamp Cottonwood | *Populus heterophylla* | 14.3 | 1 |
| 707 | Silver Maple | *Acer saccharinum* | 24.4 ± 6.9 | 4 |
| 708 | Red Maple | *Acer rubrum* | 18.8 ± 7.2 | 78 |
| 801 | Sugar Maple | *Acer saccharum* | 21.8 ± 8.1 | 40 |
| 802 | Black Cherry | *Prunus serotina* | 19.7 ± 7.5 | 77 |
| 805 | Basswood | *Tilia americana* | 31.0 ± 9.6 | 38 |
| 901 | Aspen | *Populus grandidentata* | 19.5 ± 6.2 | 6 |
| 902 | Paper Birch | *Betula papyrifera* | 19.5 ± 10.4 | 14 |
| 903 | Gray Birch | *Betula populifolia* | 17.0 ± 0.1 | 2 |
| 912 | Bigleaf Maple | *Acer macrophyllum* | 29.5 | 1 |
| 922 | California Black Oak | *Quercus kelloggii* | 9.8 ± 1.9 | 2 |
| 924 | Blue Oak | *Quercus douglasii* | 7.7 ± 0.3 | 2 |

[a]Original data from *Cavender-Bares et al.* [2006]; *Cornelissen et al.* [2003]; *Cornwell et al.* [2006]; *Medlyn and Jarvis* [1999]; *Kattge et al.* [2009]; *Kleyer et al.* [2008]; *Laughlin et al.* [2010]; *Medlyn et al.* [2001, 1999]; *Meziane and Shipley* [1999]; *Niinemets* [1999, 2001]; *Ordoñez et al.* [2010]; *Pakeman et al.* [2009]; *Poorter et al.* [2009a, 2009b]; *Preston et al.* [2006]; *Reich et al.* [2008]; *Shipley* [2002]; *Shipley and Vu* [2002]; *Wright et al.* [2006, 2004] provided via the TRY initiative.

[b]The code follows the definition by *Ruefenacht et al.* [2008]; "Std" stands for one standard errors; for species with sample = 1, the relative error is set to 20%.

developed weighted averages for the 1st and 2nd NPP components for each forest type group according to their age and area in all regions. The result is shown in the lower part of each panel in Figures 2a, 2b, and 2c.

[45] Four forest type groups (Douglas-fir, Hemlock-Sitka spruce, Loblolly shortleaf pine, Longleaf-slash pine) have "high productivity and management intensity" sub-groups; these managed forest sub-groups have a sharp increase and decline in their increment in total biomass-age relationships when compared to their more aggregated groups. Their NPP can be 2∼3 times greater than the aggregated types in the

**Table 2b.** Specific Leaf Area ($m^2$ $kg^{-1}$) for Several Forest Types

| Type | Latin Names | SLA | Samples |
|---|---|---|---|
| Fir | *Abies* | 5.1 ± 0.9 | 24 |
| Spruce | *Picea* | 5.0 ± 2.5 | 250 |
| Pine[a] | *Pinus* | 5.0 ± 1.8 | 838 |
| Hemlock | *Tsuga* | 12.3 ± 5.8 | 15 |
| Oak | *Quercus* | 13.1 ± 5.5 | 428 |
| Broadleaf[b] | | 18.9 ± 8.0 | 1338 |

[a]Set cedar SLA to pine's.

[b]Excluding the oak.

**Table 3a.** Leaf Turnover Ratio ($yr^{-1}$) for Several Forest Type Group Species[a]

| Forest Type Code | Dominant Tree Species | Latin Names | Ratio ± std | Samples |
|---|---|---|---|---|
| 101 | Jack Pine | *Pinus banksiana* | 0.272 ± 0.027 | 12 |
| 102 | Red Pine | *Pinus resinosa* | 0.455 | 1 |
| 103 | Eastern White Pine | *Pinus strobus* | 0.769 | 1 |
| 121 | Balsam Fir | *Abies balsamea* | 0.270 ± 0.005 | 6 |
| 123 | Red Spruce | *Picea rubens* | 0.126 ± 0.033 | 4 |
| 161 | Loblolly Pine | *Pinus taeda* | 0.628 ± 0.232 | 7 |
| 163 | Virginia Pine | *Virginia Pine* | 0.588 | 1 |
| 167 | Pitch Pine | *Pinus rigida* | 0.321 ± 0.065 | 4 |
| 201 | Coast Douglas-Fir | *Pseudotsuga menziesii* | 0.268 ± 0.082 | 17 |
| 221 | Ponderosa Pine | *Pinus ponderosa* | 0.421 ± 0.049 | 4 |
| 261 | White Fir | *Abies concolor* | 0.244 | 1 |
| 263 | Noble Fir | *Abies procera* | 0.182 | 1 |
| 264 | Pacific Silver Fir | *Abies amabilis* | 0.070 ± 0.033 | 2 |
| 268 | Subalpine Fir | *Abies lasiocarpa* | 0.227 | 1 |
| 301 | Western Hemlock | *Tsuga heterophylla* | 0.294 | 1 |

[a]For species with sample = 1, the relative error is set to 10%.

middle-ages. However, we did not derive separate NPP-age relationships because we lacked a spatial distribution map for managed forests to identify their locations.

### 4.3. The LAI-Age Relationships

[46] Forest cover at 30% is used as the cutoff point to determine if a pixel is forest [*Lund*, 2006]. To remove noise in the LAI-age relationships, the LAI values associated with std_age >30 years and with VCF < 0.3 were excluded from the analysis. LAI values with lower std_age (<5 years) were primarily used. Excluding forest pixels with VCF < 0.3 in the calculation may improve the LAI-age curve formation, although it may also leave out sparsely stocked forest: there are age groups with samples <100, usually for older groups, not used in the analysis (see the auxiliary material for more details).[1] We tested for exclusion of sparsely stocked forest using LAI data in version 1 and found that the screening using VCF < 0.3 or VCF < 0.1 only slightly affected LAI values in the LAI-age curve (<0.4) except for the Pinyon-Juniper forest group (an increase of LAI from 1.0 to 2.0, but this type is not included in the stock tables by *Smith et al.* [2006]), the Western Oak Group (an increase of 0.8), and the Elm/Ash/Cottonwood group (an increase of 1.0).

[47] We found that there are too many pixels with LAI values close to 6.0 for deciduous broad leaved forest in NA in the LAI product (version 1). This is because we previously set LAI maximum to 6.0 for deciduous forest in order to avoid saturation in the reduced simple ratio (RSR) signals. To assess if this saturation of RSR could distort the shape of the LAI-age curve, we tested LAI data in version 2 and version 3. Comparing the unsmoothed LAI (version 2) to the smoothed LAI (version 3), the LAI-age curve shapes for the NA forest do not change except when the values of mean unsmoothed LAI are generally greater than the smoothed LAI by about 1.0, which is understandable because the smoothing may reduce noise in the maximum LAI values. A comparison of the LAI-age curve shapes in version 1 to version 2 shows that there are no differences between the two data set except for maple-beech-birch in version 2, in which the LAI linearly increases from 6.2 (age 0) to 8 (age 130) while is confined to ~6.0 for ages 0~130 in version 1.

[48] We also examined the maximum LAI in year 2000 from MODIS [*Yang et al.*, 2006], using the same approach to derive the LAI-age relationship. The comparison shows that maximum LAI from MODIS is generally higher in the Rocky Mountains where vegetation is dominated by low LAI shrubs [*Pisek and Chen*, 2007]. However, for the forest areas where LAI is high, the LAI-age curves from the MODIS data are generally below the curves from SPOT VGT data. The LAI–age shapes are similar for the two products except for alder-maple forest: the LAI-age curves derived from SPOT VGT data show obvious peak ages, while curves derived from the MODIS data show declining form. Apparently, the version 1 product based on SPOT-VGT data provides the most reasonable LAI values, thus was chosen for the analysis of this study.

[49] In the upper part of each panel in Figures 2a, 2b, and 2c, the total LAI ($LAI_t$ in the legend) is shown in dots along with its one standard deviation. The total LAI does not increase from 0 for age zero. The separated $LAI_u$ (the upper triangle, LAI-u) and $LAI_f$ (the square, LAI-f) are shown in the upper part of each panel in Figures 2a, 2b, and 2c. The $LAI_u$ shows a rapid decrease during the early developing stage of a forest. We set $LAI_u$ = 0.21 for ponderosa pine group when stand age is greater or equal to 35, according to the measurements (the average from different plots) by *Law et al.* [2003], because there is no real solution for equation (4) for this forest type.

[50] Of the 18 forest type groups, six groups (Douglas-fir, Fir/Spruce/Mountain Hemlock, Lodgepole Pine, Hemlock/Sikta Spruce, Aspen/Birch, Alder/Maple) show a decline of LAI in mature ages coinciding with a decline in $\Delta B$; five groups (White/Red/Jack pine, Longleaf/Slash Pine, Oak/Pine, Oak/Hickory, and Oak/Gum/Cypress) show that LAI slightly increases with age after maturity; and the other seven groups show no obvious LAI change in their mature

**Table 3b.** Leaf Turnover Ratio ($yr^{-1}$) for Major Forest Types[a]

| Type | Ratio | Samples |
|---|---|---|
| Fir | 0.238 ± 0.076 | 45 |
| Spruce | 0.200 ± 0.090 | 14 |
| Pine | 0.395 ± 0.156 | 66 |
| Hemlock | 0.293 ± 0.064 | 4 |

[a]Set leaf turnover ratio of Deciduous Broad-Leaved forest to 1.0.

[1]Auxiliary materials are available in the HTML. doi:10.1029/2010GB003942.

**Table 4a.** New Fine Root C to New Leaf C Allocation Ratio (FRC/LC) (kg C kg $C^{-1}$) for Several Forest Type Groups[a]

| Forest Type Code | Dominant Tree Species | Latin Names | FRC/LC ± std | Samples |
|---|---|---|---|---|
| 102 | Red Pine | *Pinus resinosa* | 0.872 | 1 |
| 103 | Eastern White Pine | *Pinus strobus* | 0.994 | 1 |
| 142 | Slash Pine | *Pinus elliottii* | 1.09 | 1 |
| 161 | Loblolly Pine | *Pinus taeda* | 1.76 | 1 |
| 201 | Coast Douglas-Fir | *Pseudotsuga menziesii* | 2.308 ± 2.070 | 8 |
| 281 | Lodgepole Pine | *Pinus contorta* | 3.343 ± 1.692 | 4 |
| 301 | Western Hemlock | *Tsuga heterophylla* | 0.294 | 1 |
| 504 | White Oak | *Quercus alba* | 1.270 | 1 |
| 505 | Northern Red Oak | *Quercus rubra* | 1.390 | 1 |

[a]For species with sample = 1, the relative error is set to 30%.

ages. We noticed that the Deciduous Broad-leaved Forests generally have a more level LAI-age relationship than the Evergreen Needle-leaved Forests.

[51] For the three major forest biomes in the U.S. (Figure 2c) the LAI-age curve for ENF shows a declining pattern, but there are no evident declines for DBF and MF.

### 4.4. The NPP-Age Relationships

[52] The NPP-age relationships for 18 forest type groups are shown in the lower panel of Figures 2a and 2b. The regression coefficients for equation (7) are shown in Table 6.

[53] Our results show that California mixed forests have continuously increasing NPP with stand age, the Ponderosa Pine group shows no obvious NPP change after the middle-ages, and all of the other 16 forest type groups show NPP declines after their middle-age.

[54] All NPP-age relationships for the 18 forest type groups are shown in Figure 3 for comparison. In the early stand ages, forest NPP increases rapidly. The increase rate is highly dependent on the geographical location or the annual temperature and total precipitation. Lodgepole Pine in the Northern Prairie States (NPS) and North Rocky Mountain (RMN) has the lowest growth rate; the Loblolly/Shortleaf Pine, Elm/Ash/Cottonwood, Oak/Pine, and Oak/Hickory in the Southeast (SE) have the highest growth rates. Generally the growth rates are higher in regions with higher annual temperature and total precipitation: the highest rates are in the SE, South Central (SC), Northeast (NE), and Pacific Northwest regions, and the lowest growth rates are in the RMN, South Rocky Mountain (RMS), and NPS regions.

[55] The NPP reaches a peak in middle stand ages, which range from 10 years in the Southeast to 45 years in the Northwest. The DBFs generally reach a peak at 10 years in the SE, with the peak increasing to 35 years with increasing latitude along the east coast. The ENFs, Longleaf/Slash pine and Loblolly/Shortleaf Pine groups in the SE, have peak NPP values at a stand age of about 15 years; the White/Red/Jack Pine group at about 25 years; and the Spruce/Fir group at about 35 years. In the western U.S., the stand age with peak NPP ranges from 30 to 45 years, increasing with latitude.

[56] In the mature ages, the total NPP ranges from 4∼9 t C $ha^{-1}$ $yr^{-1}$. NPP declines sharply for ENF, but remains steady for DBF in mature ages.

[57] Figure 4 shows NPP normalized against the peak NPP for each type. *Gower et al.* [1996] stated that the aboveground NPP (ANPP) commonly reaches a maximum in young forest stands and decreases by 0–76% as stands mature; our results show decreases of 0∼70%, which is similar. Loblolly/Shortleaf Pine in the southeast U.S. shows remarkably high NPP because most of the forests are managed plantations: the NPP estimates are comparable to the results by *Jenkins et al.* [2001] and *McNulty et al.* [1996a, 1996b].

[58] For the three major forest biomes in the U.S. (Figure 2c), the shape of the NPP-age curve for ENF seems to be more affected by ages than the other two functional types. DBF and MF appear to be more stable and have higher NPP than the ENF through the mature ages.

### 4.5. The Uncertainty

[59] The accuracy of the derived relationships is affected by errors and uncertainties in the data sources. The relative errors of both $\Delta B$ and $M$ are 15% at 95% confidence levels (equivalent to 15%/1.95996 for a standard deviation, or 68% confidence levels, for a normal distribution) [*Heath and Smith*, 2000], so $\sigma_{\Delta B} = \Delta B \cdot 7.65\%$, and $\sigma_M = M \cdot 7.65\%$. $\sigma_{SLA}$, $\sigma_{t_l}$, and $\sigma_{R_{fr,l}}$ are from Table 5. We assumed that the relative error for $c$ is 5% based on the range of values reported in the literature.

[60] The LAI algorithm error can be estimated using the coefficient of variation of the root mean squared error, CV(RMSE). For the LAI map derived from VGT data, the CV(RMSE) for the original LAI method is 34.8% (1.27/3.65) (see Table 4 in *J. M. Chen et al.* [2002] for Canada), the CV(RMSE) for the improved LAI method is 25.8% on average (see Table 2 in *Deng et al.* [2006] for Canada), and the average CV(RMSE) for four BigFoot sites (three sites for U.S. and one site for Canada) is 24.9% [*Pisek and Chen*, 2007]. According to equation (12), the LAI algorithm error is already partial included in $\sigma_{LAI_s}$. If $\sigma_{LAI_s}$. is less than 25%, we set it to 25%, $\sigma_{LAI_a}/LAI_t$ usually is far below 10%.

[61] The absolute errors of NPP are shown in Figures 2a, 2b, and 2c, and the average relative error (E%) in the NPP-age relationship is also listed in Table 6 (ranging from 14% to 75%). The errors are mainly from the estimated root and foliage carbon. For example, the Ponderosa Pine, Lodgepole Pine, and California Mixed Conifer groups have the largest relative error because of the large errors in either SLA or $R_{fr,l}$. In contrast, the Hemlock/Sitka Spruce, and Alder/Maple

**Table 4b.** New Fine Root C to New Leaf C Allocation Ratio (FRC/LC) (kg C kg $C^{-1}$) for Major Forest Types[a]

| Forest Type | FRC/LC | Samples |
|---|---|---|
| Fir and Spruce | 1.534 ± 1.021 | 8 |
| Pine | 1.637 ± 1.354 | 17 |
| Deciduous | 1.239 ± 0.375 | 9 |

[a]Set ratios of hemlock, tamarack, and cedar to 1.59.

**Table 5.** The Area Weighted Coefficients for 18 Forest Type Groups and Three Major Forest Types in the United States

| Forest Type Code | Dominant Tree Species | Leaf Turnover Rate | FRC/LC | SLA[a] |
|---|---|---|---|---|
| 100 | White/Red/Jack Pine | 0.50 ± 0.029 | 1.18 ± 0.338 | 5.47 ± 0.96 |
| 120 | Spruce/Fir | 0.29 ± 0.026 | 1.55 ± 0.404 | 4.56 ± 0.581 |
| 140 | Longleaf/Slash Pine | 0.40 ± 0.134 | 1.17 ± 0.345 | 3.55 ± 0.683 |
| 160 | Loblolly/Shortleaf Pine | 0.62 ± 0.217 | 1.75 ± 0.496 | 6.04 ± 2.058 |
| 200 | Douglas-fir | 0.27 ± 0.082 | 2.31 ± 2.070 | 6.50 ± 2.599 |
| 220 | Ponderosa Pine | 0.42 ± 0.047 | 1.64 ± 1.285 | 2.62 ± 1.330 |
| 260 | Fir/Spruce/Mountain Hemlock | 0.25 ± 0.042 | 1.54 ± 0.493 | 5.50 ± 0.960 |
| 280 | Lodgepole Pine | 0.40 ± 0.156 | 3.34 ± 1.693 | 3.8 ± 0.600 |
| 300 | Hemlock/Sitka Spruce | 0.29 ± 0.026 | 1.59 ± 0.423 | 12.40 ± 4.755 |
| 370 | California Mixed Conifer | 0.40 ± 0.156 | 1.64 ± 1.354 | 5.03 ± 1.800 |
| 400 | Oak/Pine | 0.44 ± 0.091 | 1.57 ± 0.790 | 6.91 ± 0.870 |
| 500 | Oak/Hickory | 1.00 ± 0 | 1.24 ± 0.206 | 14.56 ± 2.845 |
| 600 | Oak/Gum/Cypress | 1.00 ± 0 | 1.24 ± 0.207 | 16.96 ± 3.407 |
| 700 | Elm/Ash/Cottonwood | 1.00 ± 0 | 1.24 ± 0.268 | 19.50 ± 5.699 |
| 800 | Maple/Beech/Birch | 1.00 ± 0 | 1.24 ± 0.297 | 22.07 ± 6.414 |
| 900 | Aspen/Birch | 1.00 ± 0 | 1.24 ± 0.343 | 19.49 ± 5.687 |
| 910 | Alder/Maple | 1.00 ± 0 | 1.24 ± 0.375 | 29.5 ± 5.900 |
| 920 | Western Oak | 1.00 ± 0 | 1.24 ± 0.205 | 12.77 ± 2.984 |
| DBF | Deciduous Broad-Leaved Forest | 1.00 ± 0 | 1.24 ± 0.105 | 19.27 ± 5.51[b] |
| ENF | Evergreen Needle-Leaved Forest | 0.26 ± 0.033[c] | 1.59 ± 0.319 | 5.67 ± 2.58[d] |
| MF | Mixed Forest | 0.63 ± 0.020 | 1.41 ± 0.199 | 10.96 ± 7.82[e] |

[a]SLA unit is in $m^2kg^{-1}$.
[b]Average from code 500 to 920.
[c]From *White et al.* [2000].
[d]Average from code 100 to 400.
[e]Average from code 100 to 920.

groups have the smallest relative errors due to the big proportion of carbon in live biomass. While the mean value in the NPP-age relationships represents a regional average, the relative error is useful to illustrate the boundaries of NPP for a stand age given the uncertainties (and/or ranges) of all the inputs.

[62] The forest stand age map is composed of pixels with 1 km resolution, but is actually interpolated from sample plot data. Therefore, the map may capture forest age distribution over landscapes but miss the age variation at smaller scales. A close check of std_age for needle-leaved forest age groups shows that most of the std_ages are less than 15 yrs except for some elder forest groups; for broad-leaved forest age groups, the std_ages are generally less than 10 yrs. For Douglas-fir, Oak/Hickory, and Maple/Beech/Birch groups, the std_ages are generally less than 5 yrs. Overall the forest age map is not a significant source of uncertainty (see the auxiliary material).

[63] We found that the maximum LAI for some DBFs is confined to ~6.0 and the associated one standard deviation is less than 1.5, likely due to limited capability of optical remote sensing to detect higher LAI because of signal saturation. We tested three different versions of LAI products but found no obvious effects on LAI-age curves. To some extent, this data limitation might have contributed to the flat pattern of the DBF LAI-age relationships in the middle stand ages. However, removing the saturated LAI values would not improve the accuracy of NPP-age curves, since it would obviously underestimate leaf carbon. In the uncertainty analysis we set the relative error of LAI to be at least 25% to assess the errors due to saturation.

[64] In this study the derived NPP-age relationships are limited to a maximum stand age of 125 years because the small numbers of pixels available for the older age groups would produce large uncertainties in the results. Caution should be taken if extrapolating the results beyond 125 years. *Lichstein et al.* [2009] found that for most North American forest types, biomass of older forests was stable or increasing, indicating an equilibrium status of old-growth forests with only slightly positive NPP. We used only one curve shape (equation (7)) for data fitting, so for some forest type groups, the curve shapes in the older ages may not be well represented and could be biased. According to the $R^2$ (coefficient of determination) and RMSE (root mean squared error) shown in Table 6, equation (7) is statistically good enough to fit the NPP-age data.

[65] The LAI-age curve shape defines the foliage (and fine root) NPP-age curve shapes. By separating the understory LAI from total LAI, we explicitly extracted understory NPP from the total tree NPP, which enabled us to develop more specific NPP-age relationships for canopy trees. This difference should be considered when using the NPP-age relationships for modeling either forest ecosystem NPP or only tree NPP.

[66] In a related study, the NPP-age relationships developed here were used as a core component in the Integrated Terrestrial Ecosystem Carbon Model (InTEC) [*Chen et al.*, 2000; *Zhang et al.*, 2012]. The modeled results of net

**Figure 2a.** LAI-age and NPP-age relationships for 18 forest type groups in U.S. (part 1/2). In the upper part of each panel, the total LAI (dots along with error bars representing one standard deviation) is shown as the sum of the understory LAI (upper triangle) and the forest LAI (squares). In the lower part of each panel, the total NPP (circles) is shown as the sum of the individual components, including biomass accumulation (cross-dotted line), mortality (dotted line), foliage turnover (plus-dotted line), and, fine root turnover (diamond-dotted line). The fitted curve for total NPP is shown as the solid line.

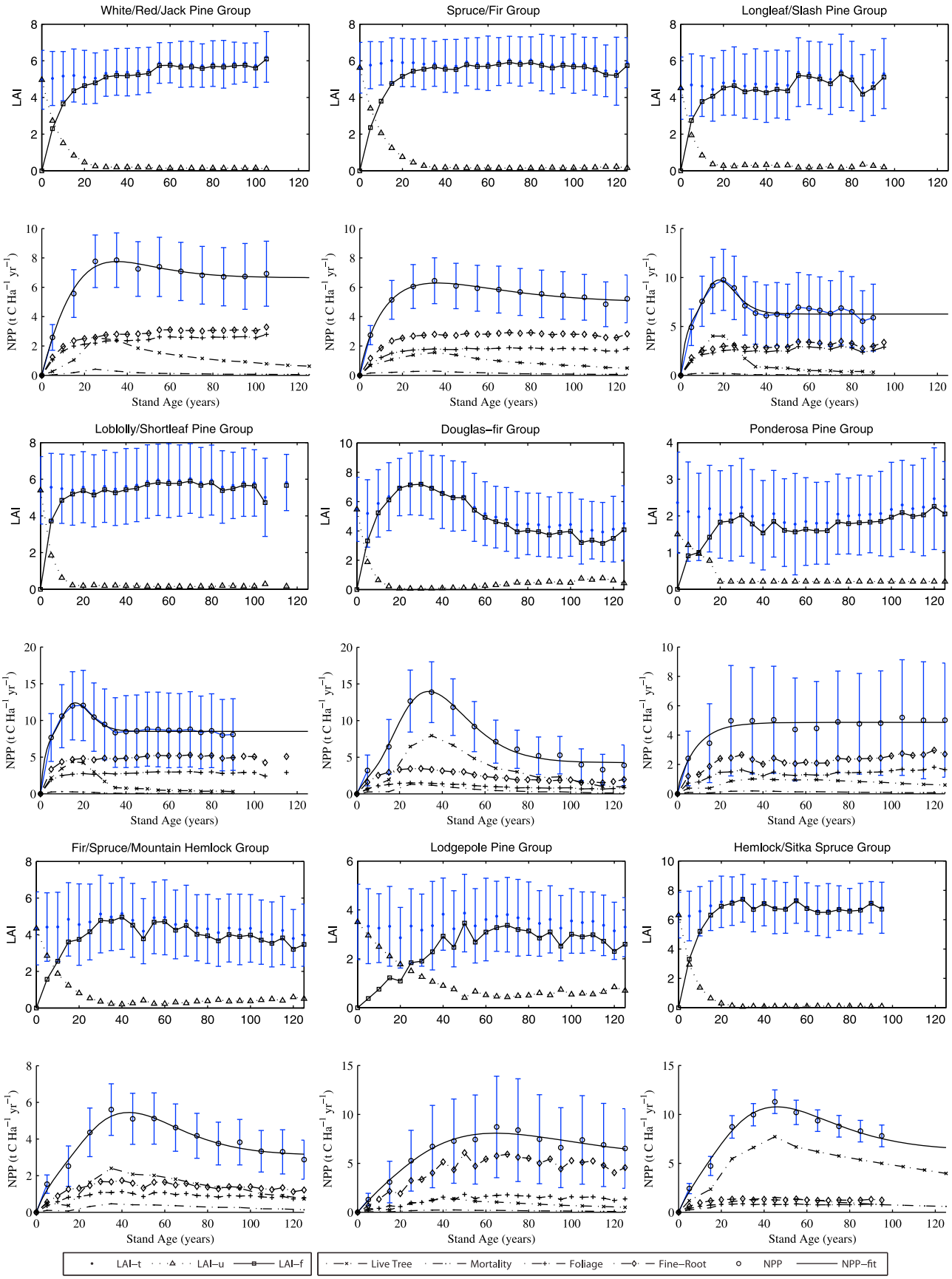
White/Red/Jack Pine Group
Spruce/Fir Group
Longleaf/Slash Pine Group
Loblolly/Shortleaf Pine Group
Douglas–fir Group
Ponderosa Pine Group
Fir/Spruce/Mountain Hemlock Group
Lodgepole Pine Group
Hemlock/Sitka Spruce Group
LAI
NPP (t C Ha$^{-1}$ yr$^{-1}$)
Stand Age (years)
LAI–t
LAI–u
LAI–f
Live Tree
Mortality
Foliage
Fine–Root
NPP
NPP–fit

**Figure 2a**

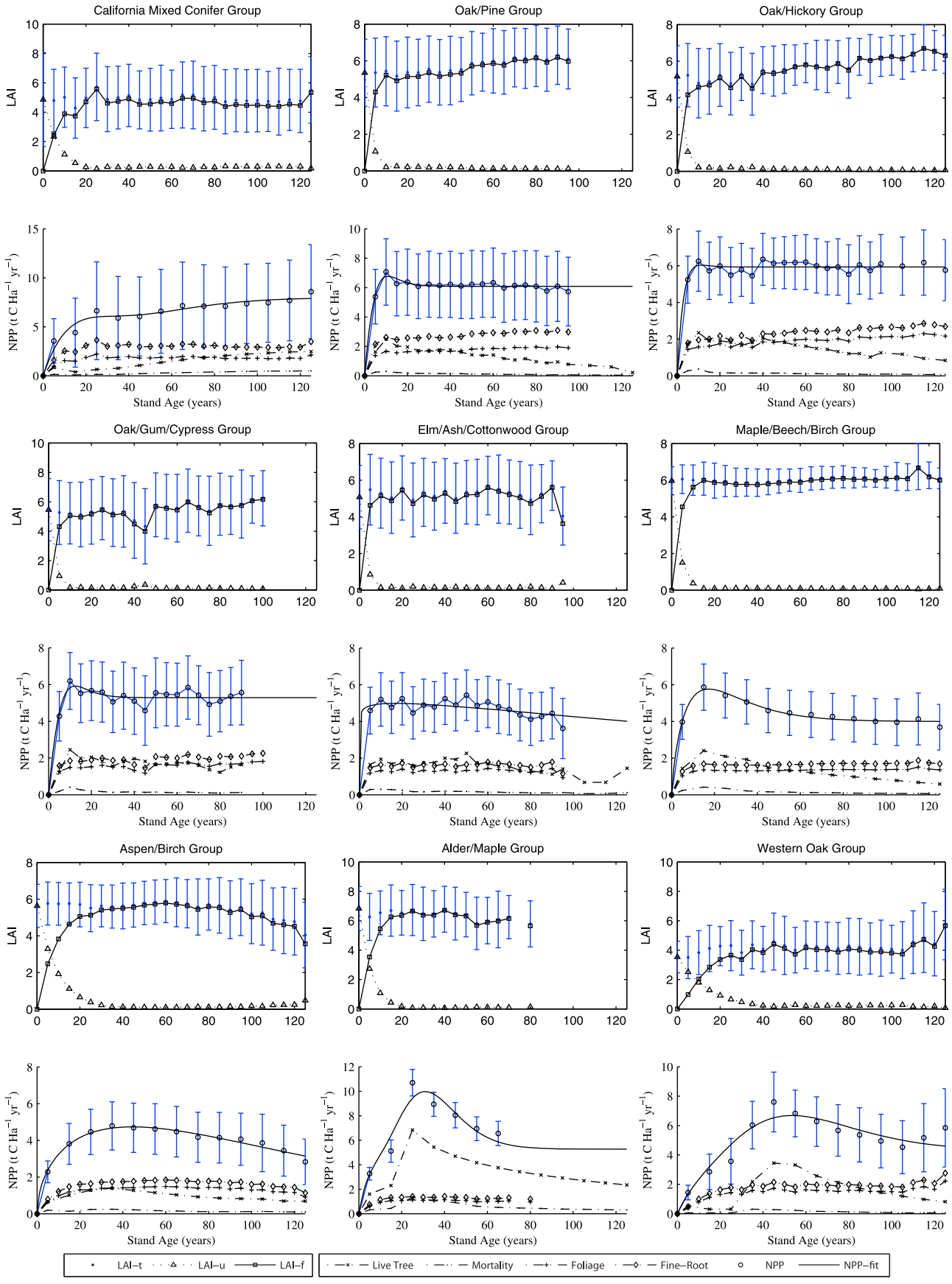


**Figure 2b.** LAI-age and NPP-age relationships for 18 forest type groups in U.S. (part 2/2).

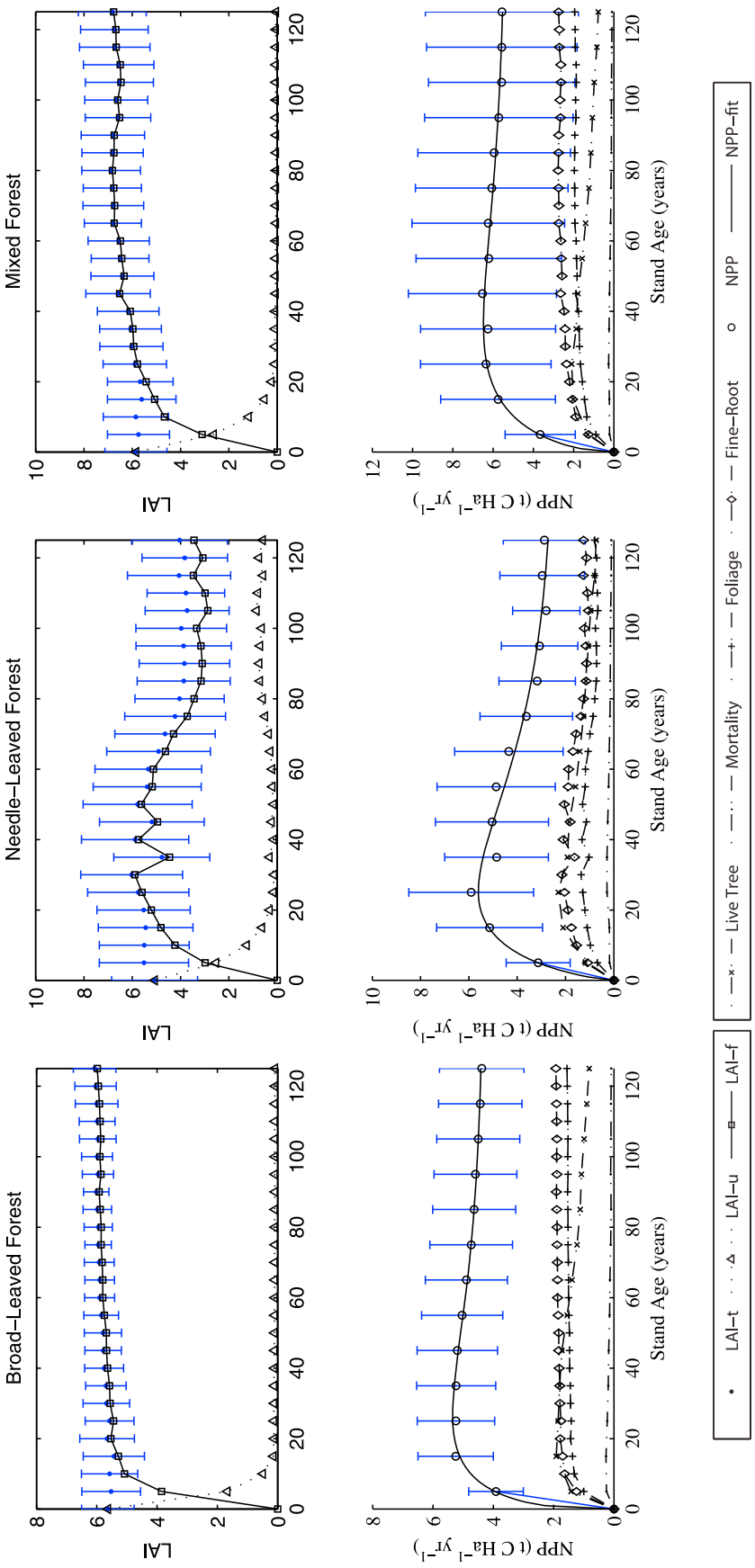


**Figure 2c.** LAI-age and NPP-age relationships for three major forest types in U.S.

**Table 6.** The Four Regression Coefficients for Equation (7) for the 18 Forest Type Groups and Three Major Forest Types in the United States[a]

| Forest Type Code | Coefficients | | | | $R^2$ | RMSE | E% |
|---|---|---|---|---|---|---|---|
| | a | b | c | d | | | |
| 100 | 6.6493 | 0.2565 | 11.0371 | 2.5657 | 0.99 | 0.19 | 29 |
| 120 | 4.9382 | 1.6194 | 25.0822 | 0.7847 | 0.99 | 0.12 | 27 |
| 140 | 6.2667 | 0.0014 | 2.6836 | 6.6742 | 0.96 | 0.39 | 47 |
| 160 | 8.4981 | 0.0011 | 2.4217 | 6.7088 | 0.99 | 0.25 | 53 |
| 200 | 4.2524 | 0.2189 | 7.3591 | 4.5542 | 0.98 | 0.51 | 48 |
| 220 | 4.8650 | 0.0686 | 8.9687 | 0.0007 | 0.96 | 0.28 | 75 |
| 260 | 3.1092 | 0.1308 | 10.1712 | 4.1608 | 0.98 | 0.22 | 32 |
| 280 | 5.4675 | 0.4737 | 20.8383 | 2.8267 | 0.98 | 0.36 | 61 |
| 300 | 6.3055 | 0.3148 | 12.7187 | 3.4731 | 0.99 | 0.36 | 14 |
| 370 | 7.9785 | −0.0690 | 12.1156 | 3.6281 | 0.95 | 0.46 | 63 |
| 400 | 6.0848 | 0.1876 | 3.2401 | 2.5745 | 0.98 | 0.18 | 37 |
| 500 | 5.9312 | 0.0897 | 2.7146 | 2.2133 | 0.96 | 0.24 | 26 |
| 600 | 5.2847 | 0.2301 | 3.8393 | 2.4410 | 0.95 | 0.29 | 32 |
| 700 | 0.1164 | 52.2800 | 329.7698 | 0.0505 | 0.92 | 0.31 | 30 |
| 800 | 3.9936 | 2.1627 | 14.2822 | 0.7284 | 0.99 | 0.13 | 28 |
| 900 | 0.0964 | 116.0364 | 82.5313 | 0.5315 | 0.99 | 0.13 | 33 |
| 910 | 5.2710 | 0.0130 | 5.3996 | 5.7082 | 0.94 | 0.75 | 14 |
| 920 | 4.2769 | 0.1529 | 13.4650 | 3.8476 | 0.91 | 0.60 | 35 |
| DBF | 4.3049 | 1.6541 | 29.4332 | 0.3430 | 1.00 | 0.05 | 28 |
| ENF | 2.4089 | 4.5941 | 27.3528 | 0.7160 | 0.97 | 0.23 | 50 |
| MF | 5.3331 | 1.5642 | 30.7310 | 0.4930 | 1.00 | 0.09 | 59 |

[a]The forest type group codes are same to Table 5. The $R^2$ and RMSE (root mean squared error) quantified the errors for fitting the NPP estimates to equation (4). E% denoted the average of e% for each stand age in a NPP-age curve, where e% is a standard deviation of NPP estimate for each stand age and expressed by percentage of the mean value.

ecosystem productivity (NEP) were compared by measured values from AmeriFlux sites (http://ameriflux.ornl.gov/). The InTEC model captures 83.2% of the variance in NEP for 147 site-years at 35 sites using the actual land cover types, forest stand ages and forest type groups (F. Zhang et al., Carbon balance in conterminous U.S. forests based on historic changes in climate, atmospheric composition, and disturbances, submitted to *Global Biogeochemical Cycles*, 2010), and suggested that the derived NPP-age curves are robust and valid to capture first order approximations of forest NPP dynamics with ages.

## 5. Discussion

[67] This study provides an independent and unique approach to derive a set of age-related NPP curves from landscape-scale monitoring data of forest inventories, remote sensing data, and species traits covering a broad range of forest types for a regional to continental level study. Three of the four NPP components are based on reliable monitoring products; only the calculation of fine root production is based on a first order approximation.

### 5.1. The Fine Root Production

[68] Fine root production is assumed linearly correlated to foliage production and the ratio $R_{fr,l}$, invariant with age. These assumptions are critical to the established NPP-age relationships. However, the correlation between new foliage carbon and new fine root carbon is supported by

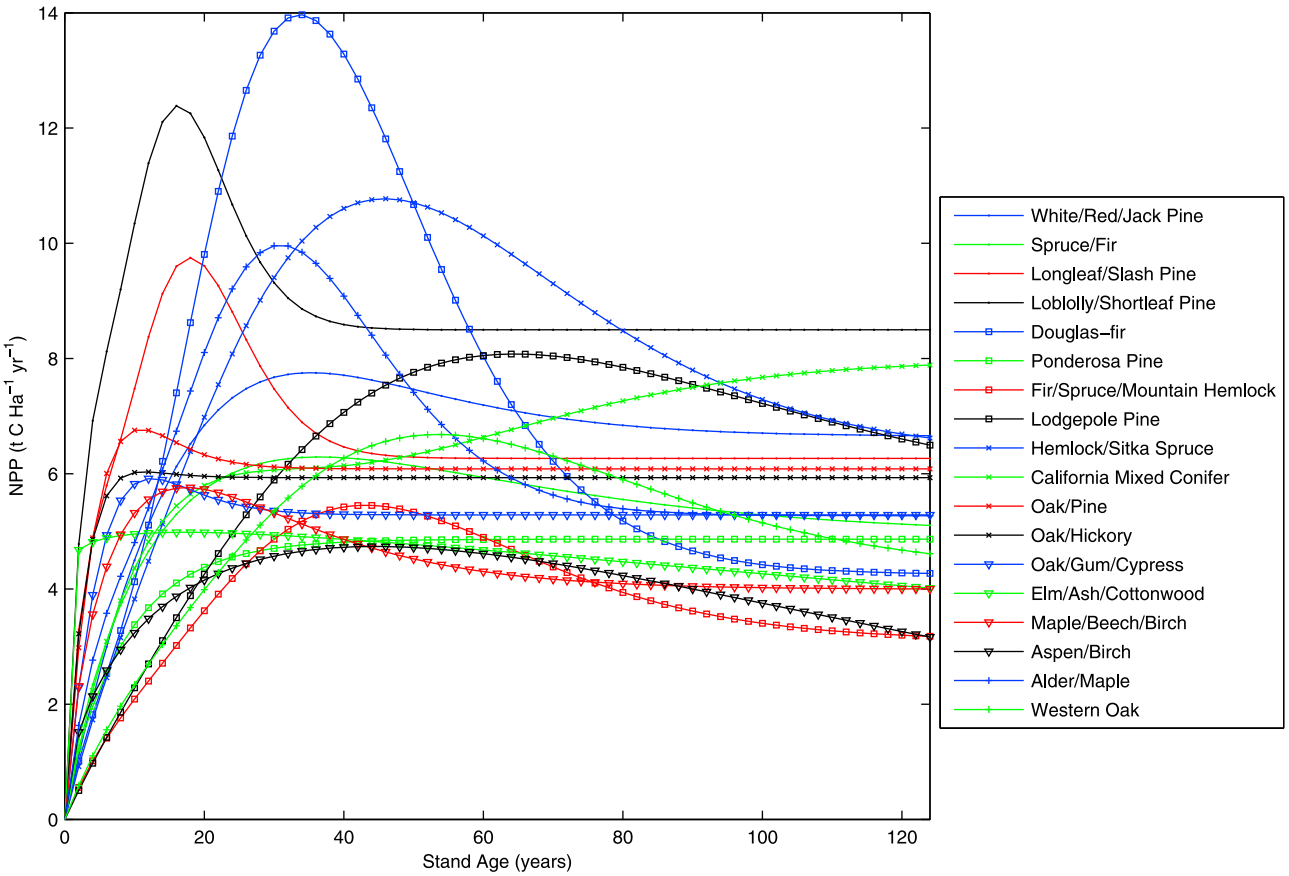


**Figure 3.** NPP-age relationships for the 18 major forest type groups within the U.S.

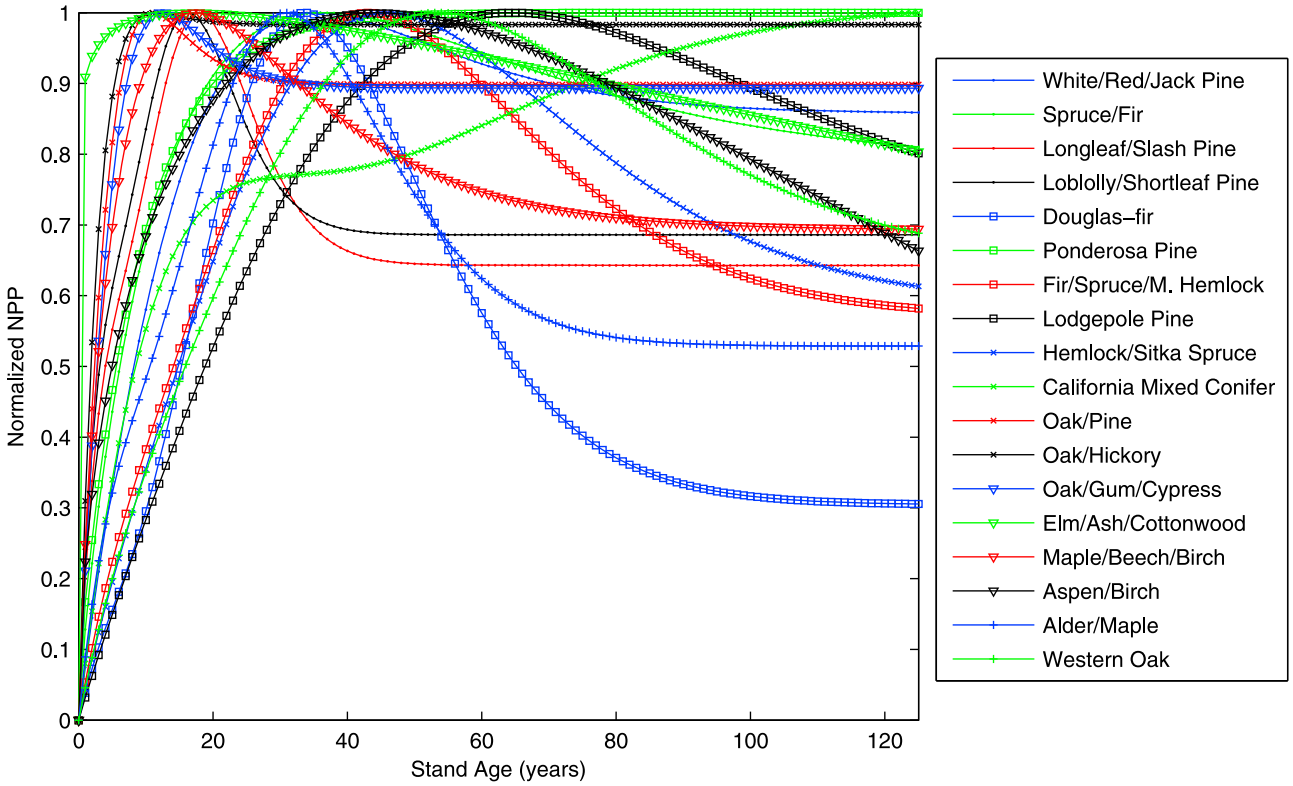


**Figure 4.** Normalized NPP-age relationships for the 18 forest type groups in U.S. Each NPP-age curve is normalized to its individual maximum NPP in peak age.

measurement data [*Borja et al.*, 2008; *Burkes et al.*, 2003; *Claus and George*, 2005; *DesRochers and Lieffers*, 2001] and is used in different models [*Chen et al.*, 2003; *Jenkins et al.*, 2003; *Pedersen*, 1998]. A recent review shows that carbon allocation to foliage, wood, roots and respiration all increased linearly with increasing GPP, implying a strong correlation between foliage and total root production [*Litton et al.*, 2007]. Since fine root production is often proportional to the total root production, an assumption of constant $R_{fr,l}$ may be reasonable. *Drake et al.* [2011] calculated fine root production for a forest dominated by loblolly pine with the assumption that the proportion of hardwood fine roots to pine fine roots was the same as the proportion of hardwood LAI to pine LAI.

[69] Carbon allocation to fine root production may have various modes [*Ryan et al.*, 1997, 2004]. For example, *Law et al.* [2003] found that the $R_{fr,l}$ was highest in youngest stands (9–23 years) in the semiarid environment in Oregon for ponderosa pine. *Yanai et al.* [2006] suggested that the fine-root biomass continues to increase past the age of canopy closure for northern hardwood stands, implying that the $R_{fr,l}$ may be greater at older ages. Fine root production can be affected by many factors [*Majdi and Andersson*, 2005; *Ruess et al.*, 1996; *Zerihun and Montagu*, 2004] and the measurement of belowground NPP is very difficult [*Gower et al.*, 1999; *Li et al.*, 2003]. These factors cause uncertainty in estimating fine root turnover, but these few case studies cannot be used to adjust our estimates because they lacking sufficient data for developing age-related ratio functions ($R_{fr,l}$) for different forest type groups across the U.S.

### 5.2. The NPP-Age Relationships and the Carbon Allocation Modes

[70] The results indicate that there are general and consistent patterns of NPP-age relationships for different forest types across the U.S., with an initial increase to a peak value, followed by a decline. The NPP-age pattern is determined by its components, first by the increment in total biomass (the mortality has a similar pattern but with smaller magnitude), then by the fine root and foliage turnover rates (which are controlled by the LAI-age pattern). The pattern is further constrained by climate conditions: the turning points of NPP-age curves and magnitude of peak values are predictably associated with the spatial distribution of temperature and precipitation for forest types. The magnitudes of peak NPP are positively correlated with the annual mean temperature and total precipitation. The results show very reasonable NPP-age patterns of tree types across geographical regions and are also consistent with those reported by *Pregitzer and Euskirchen* [2004].

[71] We compared our NPP-age relationships with similar relationships for China's forests [*Wang et al.*, 2011], where the NPP was modeled [*Liu et al.*, 1997] and validated. Five NPP-age relationships were derived for different forest ecosystems in China. Their NPP-age curves are similar to the curves derived for U.S. forests except for DBF which doesn't show a decline until age 120 yrs. However, our NPP-age relationships for some DBFs (Oak/Hickory, Oak/Gum/Cypress, and Elm/Ash/Cottonwood groups) don't show obvious declines in mature stand ages, either. This may imply that further studies should pay more attention to the DBFs.

[72] The NPP-age curve shape is dominated by the hump of wood NPP in all 18 forest types, which has a variable height and peaks at a different age for each forest type group. The foliage NPP and fine root NPP don't have such obvious humps. There are currently two hypotheses (or mechanisms) to explain the NPP-age decline: one hypothesis is that the NPP/GPP is constant, and GPP declines with age [*Drake et al.*, 2010, 2011]; the other hypothesis is that the NPP decline is caused by increasing autotrophic respiration [*Goulden et al.*, 2011]. If LAI is positively correlated with GPP, our data support the second hypothesis; however the saturation in LAI may undermine this conclusion.

[73] Our results also reveal distinct carbon allocation patterns among forest types. For instance, Loblolly/shortleaf pine has NPP mostly allocated to foliage and fine root carbon in mature ages; while Hemlock/spruce type allocated NPP mostly to the wood component. Loblolly/shortleaf pine has the maximum leaf turnover rate among all evergreen needle-leaved types (Table 5), indicating a larger carbon resource required to grow new leaves (and fine roots) as a strategy for carbon allocation in this fast growing tree type, compared with a late successional type such as hemlock/spruce.

[74] On the other hand, the Hemlock/spruce group has large SLA values and a small leaf turnover rate (Table 5), indicating that only a very small fraction of carbon is allocated to new leaves and fine roots each year, a very different carbon allocation strategy through leaf longevity and reserved resource for maintaining growth of this shade-tolerant type. The allocation ratio of its leaf NPP to total NPP (from the ninth panel of Figure 2a), shows a minimum ratio of 7.3% (at 45 yrs) and suggests a high percentage of photosynthetic product to be allocated to wood biomass.

[75] For the California mixed conifer group, which is different from all other groups, the LAI-age relationship shows a flat pattern or only a very slight decline; its NPP-age curve is dominated by the live tree biomass increment with an increasing trend. Several coniferous species in the Pacific southwest region have much longer life spans than other species in the U.S., and may take more than a century to reach maturity [*Pan et al.*, 2011a, 2011b]. This is perhaps the reason there is a continuous increasing trend of NPP in the California mixed conifer group without an obvious decline in 125 years.

## 6. Concluding Remarks

[76] In this study, we combined FIA, remote sensing and plant trait data to derive NPP-age relationships for 18 forest type groups in the United States. Each relationship represents an average estimate over broad areas for a certain forest type group.

[77] The results show that NPP of various forest type groups has a similar temporal pattern: rapid increase during early succession, peak growth in middle ages, and slow decline in mature ages. This pattern is strongly affected by mean annual temperature and total precipitation: forests in the Southeast generally show higher growth rates in younger ages, reach the peak NPP earlier, and maintain higher NPP in the mature ages, compared with forests in colder regions of the northern latitudes, high altitudes, and mid-continental areas.

[78] We also developed NPP-age relationships for the three major forest biomes: Evergreen Needleleaf Forest (ENF), Deciduous Broadleaf Forests (DBF), and Mixed Forest (MF), by further grouping the 18 forest type groups. Their NPP-age relationships show similar temporal patterns, although ENF shows a faster increase in early successional development and a faster decline in mature ages than DBF and MF. Because forest ages are limited to 125 years in this study, most of the deciduous forests in the U.S. (mostly located in the eastern U.S. such as oak-hickory, maple-beech-birch) remain very productive within this age range, while most dominant coniferous forests (i.e., loblolly pines, slash pines and Douglas-fir) have highest NPP before 50 years-old and lower productivity after the peak years. The California mixed conifer group in the Southwest is the only exception we found that shows consistently increasing NPP during the 125 years. The long life-spans of tree species in this group are likely the reason for the increasing trend of NPP.

[79] Forest management could be affecting the NPP-age curve form. In the Southeast, South Central and Pacific Northwest regions, where industrial plantations and forest management are most intensive, the biomass NPP in intensively managed sites could be 2–3 times higher than that in site with average management during the middle ages, indicating stronger carbon sequestration capacity and potential through forest management.

[80] The NPP curves derived here may have many uses for analysis of management and climate effects on the forest carbon cycle since they provide a new, independent and comprehensive source of information. For example, the NPP curves support analysis of the potential for reducing atmospheric $CO_2$ concentrations by changing the age-class structure of forested landscapes in a region. The NPP-age relationships may be incorporated in ecosystem models as key equations to project the impact of climate change on productivity, or to improve atmospheric inversion models that are used to diagnose recent changes in carbon flux over North America.

[81] **Acknowledgments.** The MODIS LAI product was downloaded from ftp://primavera.bu.edu/pub/datasets/. The VCF product (collection 4, version 3) was downloaded from http://landcover.org/data/vcf/. This study was supported by a project (2010CB950700) founded by the Global Change Program of the Chinese Ministry of Science and Technology, the Canadian Foundation for Climate and Atmospheric Sciences, and the U.S. Forest Service, Northern Research Station's climate change research program. The study has been supported by the TRY initiative (http://www.try-db.org). TRY is hosted at the Max Planck Institute for Biogeochemistry, Jena, Germany, and supported by DIVERSITAS, IGBP, the Global Land Project, QUEST and GIS "Climat, Environnement et Société" France. We are thankful to all the anonymous reviewers for constructive suggestions.

## References

Alexandrov, G. A., T. Oikawa, and G. Esser (1999), Estimating terrestrial NPP: What the data say and how they may be interpreted?, *Ecol. Modell.*, *117*(2–3), 361–369, doi:10.1016/S0304-3800(99)00019-8.

Bevington, P. R., and D. K. Robinson (2003), *Data Reduction and Error Analysis for the Physical Sciences*, McGraw-Hill, Boston, Mass.

Birdsey, R. (1996), Carbon storage for major forest types and regions in the conterminous United States, in *Forest and Global Change*, vol. 2, *Forest Management Opportunities for Mitigating Carbon Emissions. American Forests*, edited by R. N. Sampson and D. Hair, pp. 1–26, 261–379, Am. For., Washington, D. C.

Bond-Lamberty, B., W. Chuankuan, and T. G. Stith (2004), Net primary production and net ecosystem production of a boreal black spruce wildfire chronosequence, *Global Change Biol.*, *10*(4), 473–487, doi:10.1111/j.1529-8817.2003.0742.x.

Borja, I., H. A. De Wit, A. Steffenrem, and H. Majdi (2008), Stand age and fine root biomass, distribution and morphology in a Norway spruce

chronosequence in southeast Norway, *Tree Physiol.*, *28*(5), 773–784, doi:10.1093/treephys/28.5.773.

Bradford, J. B., R. A. Birdsey, L. A. Joyce, and M. G. Ryan (2008), Tree age, disturbance history, and carbon stocks and fluxes in subalpine Rocky Mountain forests, *Global Change Biol.*, *14*(12), 2882–2897, doi:10.1111/j.1365-2486.2008.01686.x.

Burkes, E. C., R. E. Will, G. A. Barron-Gafford, R. O. Teskey, and B. Shiver (2003), Biomass partitioning and growth efficiency of intensively managed *Pinus taeda* and *Pinus elliottii* stands of different planting densities, *For. Sci.*, *49*(2), 224–234.

Canadell, J. G., M. U. F. Kirschbaum, W. A. Kurz, M. J. Sanz, B. Schlamadinger, and Y. Yamagata (2007), Factoring out natural and indirect human effects on terrestrial carbon sources and sinks, *Environ. Sci. Policy*, *10*(4), 370–384, doi:10.1016/j.envsci.2007.01.009.

Carey, E. V., A. Sala, R. Keane, and R. M. Callaway (2001), Are old forests underestimated as global carbon sinks?, *Global Change Biol.*, *7*(4), 339–344, doi:10.1046/j.1365-2486.2001.00418.x.

Cavender-Bares, J., A. Keen, and B. Miles (2006), Phylogenetic structure of Floridian plant communities depends on taxonomic and spatial scale, *Ecology*, *87*(7), 109–122, doi:10.1890/0012-9658(2006)87[109:PSOFPC]2.0.CO;2.

Chapin, F. S., et al. (2006), Reconciling carbon-cycle concepts, terminology, and methods, *Ecosystems*, *9*(7), 1041–1050, doi:10.1007/s10021-005-0105-7.

Chen, J. M., and T. A. Black (1992), Defining Leaf-Area Index for non-flat leaves, *Plant Cell Environ.*, *15*(4), 421–429, doi:10.1111/j.1365-3040.1992.tb00992.x.

Chen, J., W. J. Chen, J. Liu, J. Cihlar, and S. Gray (2000), Annual carbon balance of Canada's forests during 1895–1996, *Global Biogeochem. Cycles*, *14*(3), 839–849, doi:10.1029/1999GB001207.

Chen, J. M., et al. (2002a), Derivation and validation of Canada-wide coarse-resolution leaf area index maps using high-resolution satellite imagery and ground measurements, *Remote Sens. Environ.*, *80*(1), 165–184, doi:10.1016/S0034-4257(01)00300-5.

Chen, J. M., W. M. Ju, J. Cihlar, D. Price, J. Liu, W. J. Chen, J. J. Pan, A. Black, and A. Barr (2003), Spatial distribution of carbon sources and sinks in Canada's forests, *Tellus, Ser. B*, *55*(2), 622–641, doi:10.1034/j.1600-0889.2003.00036.x.

Chen, J. M., C. H. Menges, and S. G. Leblanc (2005), Global mapping of foliage clumping index using multi-angular satellite data, *Remote Sens. Environ.*, *97*(4), 447–457, doi:10.1016/j.rse.2005.05.003.

Chen, J. M., F. Deng, and M. Z. Chen (2006), Locally adjusted cubic-spline capping for reconstructing seasonal trajectories of a satellite-derived surface parameter, *IEEE Trans. Geosci. Remote Sens.*, *44*(8), 2230–2238, doi:10.1109/TGRS.2006.872089.

Chen, W. J., J. M. Chen, D. T. Price, and J. Cihlar (2002b), Effects of stand age on net primary productivity of boreal black spruce forests in Ontario, Canada, *Can. J. For. Res.*, *32*(5), 833–842, doi:10.1139/x01-165.

Clark, D. A., S. Brown, D. W. Kicklighter, J. Q. Chambers, J. R. Thomlinson, and J. Ni (2001), Measuring net primary production in forests: Concepts and field methods, *Ecol. Appl.*, *11*(2), 356–370, doi:10.1890/1051-0761(2001)011[0356:MNPPIF]2.0.CO;2.

Claus, A., and E. George (2005), Effect of stand age on fine-root biomass and biomass distribution in three European forest chronosequences, *Can. J. For. Res.*, *35*(7), 1617–1625, doi:10.1139/x05-079.

Corless, R. M., G. H. Gonnet, D. E. G. Hare, D. J. Jeffrey, and D. E. Knuth (1996), On the Lambert W function, *Adv. Comput. Math.*, *5*(1), 329–359, doi:10.1007/BF02124750.

Cornelissen, J. H. C., B. Cerabolini, P. Castro-Díez, P. Villar-Salvador, G. Montserrat-Martí, J. P. Puyravaud, M. Maestro, M. J. A. Werger, and R. Aerts (2003), Functional traits of woody plants: Correspondence of species rankings between field adults and laboratory-grown seedlings?, *J. Veg. Sci.*, *14*(3), 311–322, doi:10.1111/j.1654-1103.2003.tb02157.x.

Cornwell, W. K., D. W. Schwilk, and D. D. Ackerly (2006), A trait-based test for habitat filtering: Convex hull volume, *Ecology*, *87*(6), 1465–1471, doi:10.1890/0012-9658(2006)87[1465:ATTFHF]2.0.CO;2.

Cramer, W., D. W. Kicklighter, A. Bondeau, B. Moore, G. Churkina, B. Nemry, A. Ruimy, A. L. Schloss, and P. P. N. M. Intercompariso (1999), Comparing global models of terrestrial net primary productivity (NPP): Overview and key results, *Global Change Biol.*, *5*, 1–15, doi:10.1046/j.1365-2486.1999.00009.x.

Deng, F., J. M. Chen, S. Plummer, M. Z. Chen, and J. Pisek (2006), Algorithm for global leaf area index retrieval using satellite imagery, *IEEE Trans. Geosci. Remote Sens.*, *44*(8), 2219–2229, doi:10.1109/TGRS.2006.872100.

DesRochers, A., and V. J. Lieffers (2001), Root biomass of regenerating aspen (*Populus tremuloides*) stands of different densities in Alberta, *Can. J. For. Res.*, *31*(6), 1012–1018.

Drake, J. E., L. M. Raetz, S. C. Davis, and E. H. DeLucia (2010), Hydraulic limitation not declining nitrogen availability causes the age-related photosynthetic decline in loblolly pine (*Pinus taeda* L.), *Plant Cell Environ.*, *33*(10), 1756–1766, doi:10.1111/j.1365-3040.2010.02180.x.

Drake, J. E., S. C. Davis, L. M. Raetz, and E. H. DeLucia (2011), Mechanisms of age-related changes in forest production: The influence of physiological and successional changes, *Global Change Biol.*, *17*(4), 1522–1535, doi:10.1111/j.1365-2486.2010.02342.x.

Fang, J. Y., and Z. M. Wang (2001), Forest biomass estimation at regional and global levels, with special reference to China's forest biomass, *Ecol. Res.*, *16*(3), 587–592, doi:10.1046/j.1440-1703.2001.00419.x.

Fogel, R. (1983), Root turnover and productivity of coniferous forests, *Plant Soil*, *71*(1–3), 75–85, doi:10.1007/BF02182643.

Global Vegetation Monitoring Unit (2003), Global Land Cover 2000 database, 28 Jan. 2010, http://bioval.jrc.ec.europa.eu/products/glc2000/glc2000.php, Eur. Comm. Joint Res. Cent., Brussels.

Goulden, M. L., A. M. S. McMillan, G. C. Winston, A. V. Rocha, K. L. Manies, J. W. Harden, and B. P. Bond-Lamberty (2011), Patterns of NPP, GPP, respiration, and NEP during boreal forest succession, *Global Change Biol.*, *17*(2), 855–871, doi:10.1111/j.1365-2486.2010.02274.x.

Gower, S. T., R. E. McMurtrie, and D. Murty (1996), Aboveground net primary production decline with stand age: Potential causes, *Trends Ecol. Evol.*, *11*(9), 378–382, doi:10.1016/0169-5347(96)10042-2.

Gower, S. T., J. G. Vogel, J. M. Norman, C. J. Kucharik, S. J. Steele, and T. K. Stow (1997), Carbon distribution and aboveground net primary production in aspen, jack pine, and black spruce stands in Saskatchewan and Manitoba, Canada, *J. Geophys. Res.*, *102*(D24), 29,029–29,041, doi:10.1029/97JD02317.

Gower, S. T., C. J. Kucharik, and J. M. Norman (1999), Direct and indirect estimation of leaf area index, $f_{APAR}$, and net primary production of terrestrial ecosystems, *Remote Sens. Environ.*, *70*(1), 29–51, doi:10.1016/S0034-4257(99)00056-5.

Grier, C. C., K. A. Vogt, M. R. Keyes, and R. L. Edmonds (1981), Biomass distribution and above-ground and below-ground production in young and mature *Abiesamabilis* zone ecosystems of the Washington Cascades, *Can. J. For. Res.*, *11*(1), 155–167, doi:10.1139/x81-021.

Hansen, M. C., R. S. DeFries, J. R. G. Townshend, R. Sohlberg, C. Dimiceli, and M. Carroll (2002), Towards an operational MODIS continuous field of percent tree cover algorithm: Examples using AVHRR and MODIS data, *Remote Sens. Environ.*, *83*, 303–319, doi:10.1016/S0034-4257(02)00079-2.

Hansen, M. C., R. S. DeFries, J. R. G. Townshend, M. Carroll, C. Dimiceli, and R. A. Sohlberg (2003), Global percent tree cover at a spatial resolution of 500 meters: First results of the MODIS vegetation continuous fields algorithm, *Earth Interact.*, *7*, 1–15, doi:10.1175/1087-3562(2003)007<0001:GPTCAA>2.0.CO;2 DOI:dx.doi.org.

Hansen, M., R. DeFries, J. R. Townshend, M. Carrol, C. Dimiceli, and R. Sohlberg (2007), Vegetation Continuous Fields MOD44B, 2000 Percent Tree Cover, collection 4, software, Univ. of Md., College Park.

He, L., J. M. Chen, S. Zhang, G. Gomez, Y. Pan, K. McCullough, and R. Birdsey (2011), Normalized algorithm for mapping and dating forest disturbances and regrowth for the United States, *Int. J. Appl. Earth Obs. Geoinformation*, *13*(2), 236–245.

Heath, L. S., and J. E. Smith (2000), An assessment of uncertainty in forest carbon budget projections, *Environ. Sci. Policy*, *3*(2–3), 73–82.

Heath, L. S., R. A. Birdsey, and D. W. Williams (2002), Methodology for estimating soil carbon for the forest carbon budget model of the United States, 2001, *Environ. Pollut.*, *116*(3), 373–380, doi:10.1016/S0269-7491(01)00213-5.

Jenkins, J. C., R. A. Birdsey, and Y. Pan (2001), Biomass and NPP estimation for the mid-Atlantic region (USA) using plot-level forest inventory data, *Ecol. Appl.*, *11*(4), 1174–1193, doi:10.1890/1051-0761(2001)011[1174:BANEFT]2.0.CO;2.

Jenkins, J. C., D. C. Chojnacky, L. S. Heath, and R. A. Birdsey (2003), National-scale biomass estimators for United States tree species, *For. Sci.*, *49*(1), 12–35.

Kattge, J., W. Knorr, T. Raddatz, and C. Wirth (2009), Quantifying photosynthetic capacity and its relationship to leaf nitrogen content for global-scale terrestrial biosphere models, *Global Change Biol.*, *15*(4), 976–991, doi:10.1111/j.1365-2486.2008.01744.x.

Kattge, J., et al. (2011), TRY - A global database of plant traits, *Global Change Biol.*, *17*(9), 2905–2935, doi:10.1111/j.1365-2486.2011.02451.x.

Kleyer, M., et al. (2008), The LEDA Traitbase: A database of life-history traits of the Northwest European flora, *J. Ecol.*, *96*(6), 1266–1274, doi:10.1111/j.1365-2745.2008.01430.x.

Kohlmaier, G. H., C. Hager, G. Wurth, M. K. B. Ludeke, P. Ramage, F. W. Badeck, J. Kindermann, and T. Lang (1995), Effects of the age class distributions of the temperate and boreal forests on the global $CO_2$

source-sink function, *Tellus, Ser. B*, *47*(1–2), 212–231, doi:10.1034/j.1600-0889.47.issue1.18.x.

Kurz, W. A., and M. J. Apps (1999), A 70-year retrospective analysis of carbon fluxes in the Canadian forest sector, *Ecol. Appl.*, *9*(2), 526–547, doi:10.1890/1051-0761(1999)009[0526:AYRAOC]2.0.CO;2.

Kutsch, W. L., C. Wirth, J. Kattge, S. Nollert, M. Herbst, and L. Kappen (2009), Ecophysiological characteristics of mature trees and stands - Consequences for old-growth forest productivity, in *Old-Growth Forest: Function, Fate and Value*, edited by C. Wirth, G. Gleixner, and M. Heimann, pp. 57–79, Springer, Berlin, doi:10.1007/978-3-540-92706-8_4.

Laughlin, D. C., J. J. Leppert, M. M. Moore, and C. H. Sieg (2010), A multi-trait test of the leaf-height-seed plant strategy scheme with 133 species from a pine forest flora, *Funct. Ecol.*, *24*(3), 493–501, doi:10.1111/j.1365-2435.2009.01672.x.

Law, B. E., O. J. Sun, J. Campbell, S. Van Tuyl, and P. E. Thornton (2003), Changes in carbon storage and fluxes in a chronosequence of ponderosa pine, *Global Change Biol.*, *9*(4), 510–524, doi:10.1046/j.1365-2486.2003.00624.x.

Le Quéré, C., et al. (2009), Trends in the sources and sinks of carbon dioxide, *Nat. Geosci.*, *2*(12), 831–836, doi:10.1038/ngeo689.

Li, Z., W. A. Kurz, M. J. Apps, and S. J. Beukema (2003), Belowground biomass dynamics in the carbon budget model of the Canadian Forest Sector: Recent improvements and implications for the estimation of NPP and NEP, *Can. J. For. Res. 33*(1), 126–136, doi:10.1139/x02-165.

Lichstein, J. W., C. Wirth, H. S. Horn, and S. W. Pacala (2009), Biomass chronosequences of United States Forests: Implications for carbon storage and forest management, in *Old-Growth Forest: Function, Fate and Value*, edited by C. Wirth, G. Gleixner, and M. Heimann, pp. 301–341, Springer, Berlin, doi:10.1007/978-3-540-92706-8_14.

Litton, C. M., J. W. Raich, and M. G. Ryan (2007), Carbon allocation in forest ecosystems, *Global Change Biol.*, *13*(10), 2089–2109, doi:10.1111/j.1365-2486.2007.01420.x.

Liu, J., J. M. Chen, J. Cihlar, and W. M. Park (1997), A process-based boreal ecosystem productivity simulator using remote sensing inputs, *Remote Sens. Environ.*, *62*(2), 158–175, doi:10.1016/S0034-4257(97)00089-8.

Lund, H. G. (2006), Definitions of forest, deforestation, afforestation, and reforestation, report, Forest Inf. Serv., Gainesville, Va. [Available from http://home.comcast.net/~gyde/DEFpaper.htm.]

Luyssaert, S., E. D. Schulze, A. Borner, A. Knohl, D. Hessenmoller, B. E. Law, P. Ciais, and J. Grace (2008), Old-growth forests as global carbon sinks, *Nature*, *455*(7210), 213–215, doi:10.1038/nature07276.

Majdi, H., and P. Andersson (2005), Fine root production and turnover in a Norway spruce stand in northern Sweden: Effects of nitrogen and water manipulation, *Ecosystems*, *8*(2), 191–199, doi:10.1007/s10021-004-0246-0.

Masek, J. G., C. Huang, R. Wolfe, W. Cohen, F. Hall, J. Kutler, and P. Nelson (2008), North American forest disturbance mapped from a decadal Landsat record, *Remote Sens. Environ.*, *112*(6), 2914–2926, doi:10.1016/j.rse.2008.02.010.

McNulty, S. G., J. M. Vose, and W. T. Swank (1996a), Potential climate change effects on loblolly pine forest productivity and drainage across the southern United States, *Ambio*, *25*(7), 449–453.

McNulty, S. G., J. M. Vose, and W. T. Swank (1996b), Loblolly pine hydrology and productivity across the southern United States, *For. Ecol. Manage.*, *86*(1–3), 241–251, doi:10.1016/S0378-1127(96)03744-9.

Medlyn, B. E., and P. G. Jarvis (1999), Design and use of a database of model parameters from elevated [$CO_2$] experiments, *Ecol. Modell.*, *124*(1), 69–83, doi:10.1016/S0304-3800(99)00148-9.

Medlyn, B. E., et al. (1999), Effects of elevated [$CO_2$] on photosynthesis in European forest species: A meta-analysis of model parameters, *Plant Cell Environ.*, *22*(12), 1475–1495, doi:10.1046/j.1365-3040.1999.00523.x.

Medlyn, B. E., et al. (2001), Stomatal conductance of forest species after long-term exposure to elevated $CO_2$ concentration: A synthesis, *New Phytol.*, *149*(2), 247–264, doi:10.1046/j.1469-8137.2001.00028.x.

Meziane, D., and B. Shipley (1999), Interacting components of interspecific relative growth rate: Constancy and change under differing conditions of light and nutrient supply, *Funct. Ecol.*, *13*(5), 611–622, doi:10.1046/j.1365-2435.1999.00359.x.

Niinemets, Ü. (1999), Research review. Components of leaf dry mass per area–thickness and density–alter leaf photosynthetic capacity in reverse directions in woody plants, *New Phytol.*, *144*(1), 35–47, doi:10.1046/j.1469-8137.1999.00466.x.

Niinemets, Ü. (2001), Global-scale climatic controls of leaf dry mass per area, density, and thickness in trees and shrubs, *Ecology*, *82*(2), 453–469, doi:10.1890/0012-9658(2001)082[0453:GSCCOL]2.0.CO;2.

Ordoñez, J. C., P. M. van Bodegom, J. P. M. Witte, R. P. Bartholomeus, J. R. van Hal, and R. Aerts (2010), Plant strategies in relation to resource supply in mesic to wet environments: Does theory mirror nature?, *Am. Nat.*, *175*(2), 225–239, doi:10.1086/649582.

Pakeman, R. J., J. Lepš, M. Kleyer, S. Lavorel, E. Garnier, and the VISTA Consortium (2009), Relative climatic, edaphic and management controls of plant functional trait signatures, *J. Veg. Sci.*, *20*(1), 148–159, doi:10.1111/j.1654-1103.2009.05548.x.

Pan, Y., J. M. Chen, R. Birdsey, K. McCullough, L. He, and F. Deng (2011a), Age structure and disturbance legacy of North American forests, *Biogeosciences*, *8*, 715–732, doi:10.5194/bg-8-715-2011.

Pan, Y. D., et al. (2011b), A large and persistent carbon sink in the world's forests, *Science*, *333*(6045), 988–993, doi:10.1126/science.1201609.

Pearson, J. A., D. H. Knight, and T. J. Fahey (1987), Biomass and nutrient accumulation during stand development in Wyoming lodgepole pine forests, *Ecology*, *68*(6), 1966–1973, doi:10.2307/1939887.

Pedersen, B. S. (1998), Modeling tree mortality in response to short- and long-term environmental stresses, *Ecol. Modell.*, *105*(2–3), 347–351, doi:10.1016/S0304-3800(97)00162-2.

Pisek, J., and J. M. Chen (2007), Comparison and validation of MODIS and VEGETATION global LAI products over four BigFoot sites in North America, *Remote Sens. Environ.*, *109*(1), 81–94, doi:10.1016/j.rse.2006.12.004.

Poorter, H., U. Niinemets, L. Poorter, I. J. Wright, and R. Villar (2009a), Erratum to "Causes and consequences of variation in leaf mass per area (LMA): A meta-analysis", *New Phytol.*, *183*(4), 1222, doi:10.1111/j.1469-8137.2009.02972.x.

Poorter, H., Ü. Niinemets, L. Poorter, I. J. Wright, and R. Villar (2009b), Causes and consequences of variation in leaf mass per area (LMA): A meta-analysis, *New Phytol.*, *182*(3), 565–588, doi:10.1111/j.1469-8137.2009.02830.x.

Pregitzer, K. S., and E. S. Euskirchen (2004), Carbon cycling and storage in world forests: Biome patterns related to forest age, *Global Change Biol.*, *10*(12), 2052–2077, doi:10.1111/j.1365-2486.2004.00866.x.

Preston, K. A., W. K. Cornwell, and J. L. DeNoyer (2006), Wood density and vessel traits as distinct correlates of ecological strategy in 51 California coast range angiosperms, *New Phytol.*, *170*(4), 807–818, doi:10.1111/j.1469-8137.2006.01712.x.

Reich, P. B., M. G. Tjoelker, K. S. Pregitzer, I. J. Wright, J. Oleksyn, and J.-L. Machado (2008), Scaling of respiration to nitrogen in leaves, stems and roots of higher land plants, *Ecol. Lett.*, *11*(8), 793–801, doi:10.1111/j.1461-0248.2008.01185.x.

Reichle, D. E., B. E. Dinger, N. T. Edwards, W. F. Harris, and P. Sollins (1973), Carbon flow and storage in a forest ecosystem, in *Carbon and the Biosphere*, edited by G. M. Woodwell and E. V. Pecan, pp. 345–365, U. S. A. E. C., Upton, N. Y.

Ruefenacht, B., et al. (2008), Conterminous U.S. and Alaska forest type mapping using forest inventory and analysis data, *Photogramm. Eng. Remote Sens.*, *74*(11), 1379–1388.

Ruess, R. W., K. VanCleve, J. Yarie, and L. A. Viereck (1996), Contributions of fine root production and turnover to the carbon and nitrogen cycling in taiga forests of the Alaskan interior, *Can. J. For. Res.*, *26*(8), 1326–1336, doi:10.1139/x26-148.

Ryan, M. G., D. Binkley, and J. H. Fownes (1997), Age-related decline in forest productivity: Pattern and process, *Adv. Ecol. Res*, *27*(27), 213–262, doi:10.1016/S0065-2504(08)60009-4.

Ryan, M. G., D. Binkley, J. H. Fownes, C. P. Giardina, and R. S. Senock (2004), An experimental test of the causes of forest growth decline with stand age, *Ecol. Monogr.*, *74*(3), 393–414, doi:10.1890/03-4037.

Schlesinger, W. H. (1997), *Biogeochemistry: An Analysis of Global Change*, 2nd ed., 588 pp., Academic, San Diego, Calif.

Shipley, B. (2002), Trade-offs between net assimilation rate and specific leaf area in determining relative growth rate: relationship with daily irradiance, *Funct. Ecol.*, *16*(5), 682–689, doi:10.1046/j.1365-2435.2002.00672.x.

Shipley, B., and T.-T. Vu (2002), Dry matter content as a measure of dry matter concentration in plants and their parts, *New Phytol.*, *153*(2), 359–364, doi:10.1046/j.0028-646X.2001.00320.x.

Smith, J. E., L. S. Heath, and J. C. Jenkins (2003), Forest volume-to-biomass models and estimates of mass for live and standing dead trees of U.S. forests, report, 57 pp., U. S. Dep. of Agric. For. Serv., Newtown Square, Penn.

Smith, J. E., L. S. Heath, K. E. Skog, and R. A. Birdsey (2006), Methods for calculating forest ecosystem and harvested carbon with standard estimates for forest types of the United States, *Gen. Tech. Rep. NE-343*, 216 pp., U. S. Dep. of Agric. For. Serv., Newtown Square, Penn.

Smith, W. B., P. D. Miles, C. H. Perry, and S. A. Pugh (2009), Forest resources of the United States, 2007. A technical document supporting the Forest Service 2010 RPA assessment, *Gen. Tech. Rep. WO-78*, U. S. Dep. of Agric. For. Serv., Washington, D. C.

Song, C. H., and C. E. Woodcock (2003), A regional forest ecosystem carbon budget model: Impacts of forest age structure and landuse history, *Ecol. Modell.*, *164*(1), 33–47, doi:10.1016/S0304-3800(03)00013-9.

Vogt, K. A., C. C. Grier, C. E. Meier, and R. L. Edmonds (1982), Mycorrhizal role in net primary production and nutrient cycling in abies-amabilis ecosystems in western Washington, *Ecology*, *63*(2), 370–380, doi:10.2307/1938955.

Wang, C., B. Bond-Lamberty, and S. T. Gower (2003), Carbon distribution of a well- and poorly drained black spruce fire chronosequence, *Global Change Biol.*, *9*(7), 1066–1079, doi:10.1046/j.1365-2486.2003.00645.x.

Wang, S., J. M. Chen, W. M. Ju, X. Feng, M. Chen, P. Chen, and G. Yu (2007), Carbon sinks and sources in China's forests during 1901–2001, *J. Environ. Manage.*, *85*(3), 524–537, doi:10.1016/j.jenvman.2006.09.019.

Wang, S. Q., L. Zhou, J. M. Chen, W. M. Ju, X. F. Feng, and W. X. Wu (2011), Relationships between net primary productivity and stand age for several forest types and their influence on China's carbon balance, *J. Environ. Manage.*, *92*(6), 1651–1662, doi:10.1016/j.jenvman.2011.01.024.

Waring, R. H., and W. H. Schlesinger (1985), *Forest Ecosystems: Concepts and Management*, Academic, San Diego, Calif.

White, M. A., P. E. Thornton, S. W. Running, and R. R. Nemani (2000), Parameterization and sensitivity analysis of the BIOME–BGC terrestrial ecosystem model: Net primary production controls, *Earth Interact.*, *4*(3), 1–85, doi:10.1175/1087-3562(2000)004<0003:PASAOT>2.0.CO;2.

White, M. A., P. E. Thornton, S. W. Running, and R. R. Nemani (2002), Literature-Derived Parameters for the BIOME-BGC Terrestrial Ecosystem Model, http://www.daac.ornl.gov, Oak Ridge Natl. Lab., Oak Ridge, Tenn.

Wright, I. J., et al. (2004), The worldwide leaf economics spectrum, *Nature*, *428*(6985), 821–827, doi:10.1038/nature02403.

Wright, I. J., P. B. Reich, O. K. Atkin, C. H. Lusk, M. G. Tjoelker, and M. Westoby (2006), Irradiance, temperature and rainfall influence leaf dark respiration in woody plants: Evidence from comparisons across 20 sites, *New Phytol.*, *169*(2), 309–319, doi:10.1111/j.1469-8137.2005.01590.x.

Yanai, R. D., B. B. Park, and S. P. Hamburg (2006), The vertical and horizontal distribution of roots in northern hardwood stands of varying age, *Can. J. For. Res.*, *36*(2), 450–459, doi:10.1139/x05-254.

Yang, W., N. V. Shabanov, D. Huang, W. Wang, R. E. Dickinson, R. R. Nemani, Y. Knyazikhin, and R. B. Myneni (2006), Analysis of leaf area index products from combination of MODIS Terra and Aqua data, *Remote Sens. Environ.*, *104*(3), 297–312, doi:10.1016/j.rse.2006.04.016.

Yarie, J., and S. Billings (2002), Carbon balance of the taiga forest within Alaska: Present and future, *Can. J. For. Res.*, *32*(5), 757–767, doi:10.1139/x01-075.

Zaehle, S., S. Sitch, I. C. Prentice, J. Liski, W. Cramer, M. Erhard, T. Hickler, and B. Smith (2006), The importance of age-related decline in forest NPP for modeling regional carbon balances, *Ecol. Appl.*, *16*(4), 1555–1574, doi:10.1890/1051-0761(2006)016[1555:TIOADI]2.0.CO;2.

Zerihun, A., and K. D. Montagu (2004), Belowground to aboveground biomass ratio and vertical root distribution responses of mature *Pinus radiata* stands to phosphorus fertilization at planting, *Can. J. For. Res.*, *34*(9), 1883–1894, doi:10.1139/x04-069.

Zhang, F., J. M. Chen, Y. Pan, R. A. Birdsey, S. Shen, W. Ju, and L. He (2012), Attributing carbon changes in conterminous U.S. forests to disturbance and non-disturbance factors from 1901 to 2010, *J. Geophys. Res.*, *117*, G02021, doi:10.1029/2011JG001930.